

Response to review comments on acp-2015-586 from reviewer 2

The original comments are provided in black, our response is given below each comment in red.

Thank you for the careful reading of our manuscript and your review.

This paper evaluates one year of a high-resolution (i.e. 12 km grid-spacing) WRF-Chem simulation over North America with observations from MODIS Aqua and Terra as well as the ground networks AERONET and EPA. The remotely sensed observations include both AOT and AE. The authors collocate the simulated data to remotely sensed data and analyse the resulting spatial patterns on monthly and yearly time-scales. The topic of the paper is entirely in line with the interests of ACP, and so publication in ACP is possible. There appears to be a serious issue though with the remotely sensed data used in the analysis: MODIS and AERONET agree even less with each other than MODIS and WRF-Chem or AERONET and WRF-Chem (Table 3, AOT column). This suggests that at least one of these remotely sensed datasets is flawed and not appropriate for the evaluation of WRF-Chem. The authors merely list this statistic but draw no conclusions from it or offer explanations of it. This issue really needs to be resolved before publication.

Thank you for your positive assessment. We have addressed the issue with the remotely sensed data in the comments below and in the manuscript.

General comments

While model evaluation with observations is very important, it is difficult to see what this paper adds besides a lot of statistics. In particular, the authors barely explore two interesting datasets: the EPA data and the Delaware gridded precip data. Some interesting questions come out of this study and addressing them might give the paper a bigger impact:

- does the model agreement with observations depend on scale? What are the length- and time-scales in the different datasets anyway? Does the model agree better after further aggregating the data over, say, 24, 48, 96 km? (Note that while pollution forecasts require spatio-temporally highly resolved simulations, forcing estimates probably can do with spatio-temporal averages)

Thanks for the useful comment. Using very limited data, prior research indicated mesoscale variability (horizontal scales of 40–400 km and temporal scales of 2–48 h) is a common and perhaps universal feature of lower-tropospheric aerosol light extinction [Anderson *et al.*, 2003]. However, to our knowledge, no prior systematic attempt has been made to quantify and test the universality of aerosol scales of coherence over the contiguous US. We have conducted some additional analyses to test the dependence of MFB on the spatio-temporal scales by aggregating the 12km grid cells (both from WRF and MODIS) to coarser resolutions (see Figure 6). When looking at monthly aggregated data we only see a slight variation of MFB during cold months when the 12km data are aggregated to a coarser resolution, possibly indicating that those months are more sensitive to biases in the chemical composition, mostly associated with underestimation of sulfate aerosols (see response to reviewer 3) and possibly also as a result of the lower data availability.

Reference:

Anderson, T. L., Charlson, R. J., Winker, D. M., Ogren, J. A., and Holmen, K.: Mesoscale variations of tropospheric aerosols, *Journal of the Atmospheric Sciences*, 60, 119-136, 10.1175/1520-0469(2003)060<0119:MVOTA>2.0.CO;2, 2003.

We added the following text:

“Using very limited data, prior research indicated mesoscale variability (horizontal scales of 40–400 km and temporal scales of 2–48 h) is a common and perhaps universal feature of lower-tropospheric aerosol light extinction [Anderson et al., 2003]. However, we are not aware of prior systematic attempts to quantify and test the universality of AOD scales of coherence over the contiguous US. To test the sensitivity of the MFB in simulated AOD to spatial aggregation, we excluded the first 12 cells to the left and to the top of the simulated domain and averaged the remaining 12×12 km grid cells over the following scales: 24×24, 36×36, 48×48, 72×72, 96×96, 144×144, 192×192, 216×216, 288×288, 384×384, 432×432, 576×576, 864×864, 1152×1152, 1728×1728, 3456×3456 km. The last spatial average corresponds to a single grid cell encompassing the entire domain (excluding the outer 12 cells located to the West and North of the simulation domain). Each spatial average at a coarser resolution is computed as the mean of all valid 12×12 km grid cells within the averaging area. We then computed the MFB for the regridded WRF-Chem and MODIS data pair and found that, on a yearly basis, MFB is highest at 12km (0.14 for Aqua and 0.15 for Terra) and reaches a first minimum at 72 km for Aqua (MFB=0.13) and 384 km for Terra (MFB=0.13) (see Fig. 6). However, the MFB and hence systematic error in AOD relative to MODIS exhibits only a weak dependence on the level of spatial aggregation.”

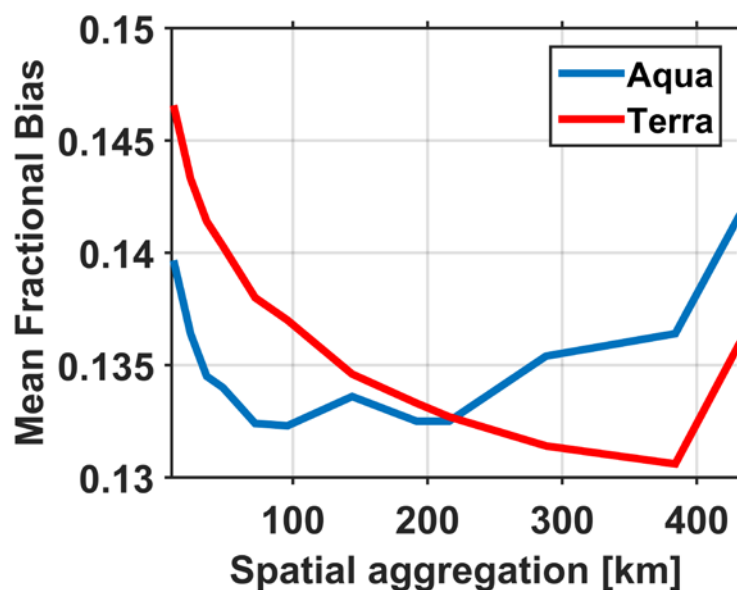


Figure 6. Mean fraction bias (MFB) on AOD from WRF-Chem as a function of spatial aggregation relative to observations from Terra (red line) and Aqua (blue line).

- Are model deviations from remotely sensed observations correlated with e.g. EPA differences or precip measurements? The paper only addresses this in the most cursory fashion. What can we learn from this about model deficiencies?

As we mentioned the AOD biases in the fall months (September and October) do appear to be linked to precipitation biases, and certainly are reflected in the near-surface PM_{2.5} concentrations and composition (Fig. S4 and Fig. 4). We now elaborate on this a little further (lines 370-376; 418-420; Figures 4 and 8).

- Are AE differences somehow correlated with AOT differences (or vice versa)? Can this be used to understand model deficiencies?

As the reviewer will know AE is very difficult to derive from the MODIS measurements and the uncertainty in AE scales with AOD (AE is very uncertain at AOD < 0.2). This

and the fact that AE is derived from wavelength dependent AOD makes the uncertainties on the measurements certainly correlated. As indicated in Figure 7, for some AERONET sites there is evidence that positive bias in AOD is associated with high negative bias in AE, but this is not uniformly the case (e.g. for the site at 77.8W 55.3N WRF-Chem exhibits positive bias in AOD across the entire pdf while the simulated AE is negative biased, but the site at 84.28W 35.95N exhibits relative good accord for AOD but is negative biased in AE almost to the same amount as the northern station).

We also added the following comment at the end of Section 3.2:

“AE is very difficult to derive from the MODIS measurements and the uncertainty in AE scales with AOD (AE is very uncertain at $AOD < 0.2$). Further, AE is derived from wavelength dependent AOD, thus the uncertainties on the measurements are certainly correlated. As indicated in Figure 7, for some AERONET sites there is evidence that positive bias in AOD is associated with high negative bias in AE, but this does not uniformly occur over eastern North America (e.g. for the site at 77.8W 55.3N WRF-Chem exhibits positive bias in AOD across the entire pdf while the simulated AE is negative biased, but the site at 84.28W 35.95N exhibits relative good accord for AOD but is negative biased in AE almost to the same amount as the northern station).”

- Why are only 12 AERONET sites used? Surely AERONET offers more over the continental USA? Possibly this is due to a very strict interpretation of Kinne et al. 2013 recommendations? We analysed data from 22 AERONET stations which are all stations collecting data during 2008 over our domain and satisfying the condition described in Section 2.2 for the comparison on a monthly basis:

“Where WRF-Chem output is compared with data from AERONET stations, a station is only included if there are at least 20 simultaneous estimates available.”

It is worthy of note that although a large number of sites in the US have seen deployment of AERONET instrumentation, relatively few have significant data availability for 2008 as shown by the figure below:

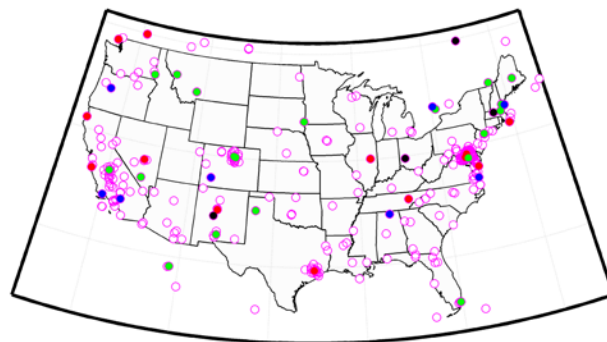


Figure. AERONET stations in/close to the contiguous US (magenta) that have been in operation as part of the network. Colors show the number of days at each station that in 2008 had > 1 observation of AOD at 440 nm (red>200, green=100-200, blue=50-100, black <50).

- Finally, the title of the paper is rather grand. A simple 'Evaluation of high-resolution WRF-Chem run over North America with remote sensing datasets' would do as well. The current title suggests a far broader canvas: multiple regional models for different domains using a set of complimentary observations beyond remote sensing data. Also, while remote sensing data

are of course appropriate for analysing forcing estimates from a model, they are by no means conclusive. The authors never really make the link to forcings.

We modified the title as follows:

Evaluating the skill of high resolution WRF-Chem simulations in describing drivers of aerosol direct climate forcing at the regional scale

Specific comments

Abstract

p 27312, l 10: MFB=0.5 is not a small bias. Even 0.17 is not a small bias, given that part of AOT is due to background and presumably constant in climate change/future predictions. Please strike 'small'.

Done

p 27312, l 15: "AE is retrieved with higher uncertainty from the remote sensing observations." does not belong here. Either strike or move one sentence.

We rephrased as follows:

"The model is biased towards simulation of coarse mode aerosols (annual MFB for AE = -0.10 relative to MODIS and -0.59 for AERONET), but the spatial correlation for AE with observations is 0.3-0.5 during most months, despite AE is retrieved with higher uncertainty from the remote sensing observations."

Introduction

p 27313, l 27: this suggests that PM10 or PM2.5 measurements have no bias and zero measurement uncertainty. This is of course not true. Please rephrase. AFAIK, IMPROVE measurements are made every 3 days, so also with PM10, PM2.5 under sampling may be an issue.

We have rephrased this:

"Long-term measurements of aerosol properties are largely confined to aerosol mass (total, PM₁₀ or PM_{2.5}) in the near-surface layer which may or may not be representative of either the total atmospheric burden (Ford and Heald, 2013;Alston et al., 2012), or radiation extinction and hence climate forcing. Further, aerosol composition measurements are often a 24-hour integrated sample taken only 1 in 3 days and thus are subject to under sampling. Hence they provide an incomplete description of temporal variability and mean aerosol burdens for model performance evaluation."

p. 27314, l. 10: These are strange references here. E.g. Spracklen et al does not really discuss spatial scales in observed aerosol. There is quite a bit of literature on this though: Anderson et al JAS 2003; Kovacs et al JGR 2006; Santese et al JGR 2007; Sinzuka & Redemann ACP 2011; Schutgens et al AMT 2013. Several of these papers deal explicitly with spatial scales in remotely sensed properties.

Thanks for the suggestions. We replaced the reference with the following:

"However, aerosol populations (and dynamics) are known to exhibit higher spatial variability (and scales) than can be manifest in those models (Kovacs et al.,2006;Kulmala et al., 2011;Santese et al., 2007; Schutgens et al., 2013;Sinzuka and Redemann, 2011)."

p 27314, l 14: "The skill of these models in reproducing the spatio-temporal variability in the aerosol size distribution, composition, concentration and radiative properties is incompletely characterized. Accordingly, there is large model-to-model variability both in the global mean

direct aerosol forcing and in the spatial distribution". Skill characterisation and model-to-model variability are unrelated. Please rephrase as these sentences are confusing.

We rephrased as follows:

“The skill of these models in reproducing the spatio-temporal variability in the aerosol size distribution, composition, concentration and radiative properties is incompletely characterized. Further large model-to-model variability both in the global mean direct aerosol forcing and in the spatial distribution thereof exists (Kulmala et al., 2011; Myhre et al., 2013) leading to high uncertainty in quantification of aerosol climate forcing.”

p 27315, l 13: "However, there are also variations in the way in which model skill is evaluated leading to ambiguity in terms of prioritizing future research directions". Even if we all use the same metric, there would still be ambiguity over e.g. what is the best way to improve models. Arguably, this is far more important than the metric itself. Please rephrase.

We rephrased as follows:

“However, there are also variations in the way in which model skill is evaluated and divergent opinions regarding prioritization of future research directions.”

p 27315, l 23: "Assessment of value added (or lack thereof) from high resolution regional vs. global coarse resolution models is not quantifiable from prior studies alone." Which prior studies are referred to? What is meant by this sentence?

We rephrased as follows:

“Assessment of value added (or lack thereof) from high resolution regional versus global coarse resolution models has not been clearly quantified in previous studies (Table 1).”

p 27316, l 4: "inferential statistics". Descriptive statistics seem more appropriate here. I find little hypothesis testing or inference in this paper.

Changed to “descriptive statistics”.

p 27316, l 9: "Prior analyses of Level-3 10 (10 resolution) MODIS AOD over the eastern half of North America have indicated the frequency of co-occurrence of extreme AOD values (>local 90th percentile) decreases to below 50% at 150 km from a central grid cell located in southern Indiana, but is above that expected by random chance over almost all of eastern North America (Sullivan et al., 2015)." What central grid-cell? I guess the authors are referring to a particular model evaluation? What is the importance of the 150 km distance? Instead of going into a lot of detail, maybe you can just tell in one or two sentences what the relevance of Sullivan 2015 is to your work?

We agree and rephrased as follows:

Prior analyses of Level-3 (1° resolution) MODIS AOD over the eastern half of North America have indicated extreme AOD values (> local 90th percentile) are coherent over regional scales (~ 150 km) (Sullivan et al., 2015). Thus, our evaluation exercise also includes an analysis of the spatio-temporal coherence of extreme events.

p 27316, l 27: Strictly speaking, AERONET measurements are not columnar measurements. Standard AERONET product measures attenuation of direct sun-light and so actually measures aerosol along a slant path. However, final AOT values are corrected for this to represent the vertical column.

Agree, we removed “columnar”.

p 27317, l 12: It is customary to have a brief overview of the paper’s structure at this point.

We added the following paragraph:

“This paper is structured as follows. We first describe the settings used in our WRF-Chem simulations and introduce the remote sensing and other data used for model evaluation (Sect. 2). A description of statistical metrics used for the evaluation is also provided. Section 3 presents results of the evaluation of simulated AOD and AE versus observations, as well as findings on extreme AOD values. In Section 4 we summarize our findings and draw conclusions.”

p 27318, l 29: Don't the median diameters of MADE aerosol vary throughout the simulation, in both space and time? Or are they fixed (i.e. is a single moment scheme used, where mass only is considered)?

Yes, diameters vary throughout the simulations (the values we reported refer to the initial diameter) whereas the standard deviations are fixed within each mode. We modified the text accordingly.

p 27320, l 7: How does this official error estimate compare with Hyer et al AMT 2011? I believe official MODIS estimates are rather optimistic.

Thanks for pointing this out. We included this reference for comparison.

“The L2 AOD uncertainty is $\pm 0.05 \pm 0.15 \times \text{AOD}$ over land relative to global sun photometer measurements from AERONET; even when no spatiotemporal averaging is used in the comparison (i.e. all combinations of MODIS retrievals within 30 km of an AERONET site and all AERONET retrievals within 30 min of the satellite overpass), 71% of MODIS retrievals fall within a $\pm 0.05 \pm 0.2 \times \text{AOD}$ envelope relative to AERONET over E. CONUS (Hyer et al., 2011).”

p 27321, l 6-19: The exact procedure is not clear due to missing information and confusing sentences. The cloud screen (presumably from MODIS?) is applied to model data first and then only cells with 5 or more observations per month are retained? Cases with cloud fraction > 0 are discarded? In my experience that removes a lot of good observations as well. Which cloud screen do you use: the one that is part of the aerosol product MYD/MOD04 or another one? What do you do with MISR data or AERONET? Model data are not masked by observation availability in their case? AERONET is compared to the closest grid-cell or do you interpolate model data to the site? What about time of observations? You choose again nearest model time?

We did not apply a cloud screen to the MODIS or MISR data, beyond what is already in the algorithms to remove cloud pixels. In the NASA products 'cloudy' pixels are identified and removed; then for the remaining pixels, the 50%/20% brightest/darkest pixels are also removed (assumed to be cloud contaminated), and the remaining pixels are averaged for the retrieval (Levy et al. 2013). So we do get good retrievals when cloud fraction > 0, but the cloud pixels are screened out.

We reworded the data section as follows:

“To avoid the discontinuity in the MODIS retrieval algorithm due to different assumed aerosol types (Levy et al., 2007), we confine our analyses of model skill to longitudes east of 98°W. Only WRF grid cells with cloud fraction = 0 during the satellite over pass of each grid cell are used in comparison to MODIS/MISR observations, and only grid cells with at least 5 valid observations (both from MODIS/MISR and cloud-screened WRF) during a given month are included in the analyses presented herein. It is worth noting that setting a threshold of 10 observations does not significantly affect the results. For a uniform assessment, L2 MODIS and L3 MISR data have been interpolated from their native grids (and resolutions of 10 km and $0.5^\circ \times 0.5^\circ$, respectively) to the WRF-Chem 12 km resolution grid by computing the mean of pixels with valid data within $0.1^\circ/0.3^\circ$ for

MODIS/MISR from the model centroids. The choice of averaging over a slightly larger area than model resolution is dictated by the sparsity of valid satellite retrievals. For AERONET vs. MODIS comparison, we only use the nearest MODIS data (after regridding to WRF) to each site. Where hourly WRF-Chem output is compared with data from AERONET sites, a station is only included if there are at least 20 simultaneous estimates available, and each AERONET measurement is compared to the nearest WRF-Chem time step and to the grid cell containing the station.”

Reference:

Levy, R. C., Mattoo, S., Munchak, L. A., Remer, L. A., Sayer, A. M., & Hsu, N. C. (2013). The Collection 6 MODIS aerosol products over land and ocean. Atmos. Meas. Tech. Discuss, 6, 159-259.

p 27321, l 23: While the use of MFB is warranted, its interpretation is less clear than (M-O)/O, please discuss this. Also, relative errors (like MFB) seem less appropriate than absolute errors in case of an intensive property like AE.

As the reviewer suggests, there are a range of performance metrics one can use to evaluate models. We decided to compute the MFB instead of Normalized Mean Bias (NMB) since NMB is biased towards overestimations and assumes observations are without error, while MFB gives equal weight to underestimation and overestimation. We put a reference to this at line 285.

p 27322, l 1-5: "Where MFB is reported for WRF-Chem vs. MODIS or MISR, C_m is the monthly mean AOD or AE simulated by WRF-Chem at a specific location, C_0 refers to the same quantify from MODIS or MISR (Table 3) and N is the sample size. Where MFB is reported in comparisons of WRF-Chem with AERONET, the monthly average in the model grid cell containing the AERONET site is compared with monthly averaged observations (C_0)." So much text suggests there is a difference in how you treat MODIS and AERONET data, yet I see no difference?

Correct, there is no big difference in the way we treat AERONET, so we reworded as follows:

“Where MFB is reported for WRF-Chem versus MODIS/ MISR/AERONET, C_m is the monthly mean AOD or AE simulated by WRF-Chem at a specific location, C_0 refers to the same quantify from remote sensing data (Table 3) and N is the sample size.”

p 27323, l 10: What is type i? Which rows and columns do you refer to? Maybe it is easier to simply mention these metrics (incl EQQ and Taylor plot) and then refer to papers, books that discuss them in more detail.

We simplified the text and removed the formula. We preferred to keep some brief explanations of the methodologies applied for clarity.

p. 27323, l 25: So ME, WN and MN are frequencies of occurrence? Occurrence itself is not a metric.

Replaced with “frequency”.

p 27324, l 10: Why are these extra metrics HR & TS useful? What do they tell you that Accuracy does not tell you? Instead of giving the functional forms (which readers can look up in books anyway) it is more useful to explain the meaning of the various metrics.

We preferred to maintain the functional forms for easier reference in the result and discussion sections. However we included a more detailed description as follows:

“The Accuracy describes the fraction of grid cells co-identified as exceeding $p75$ or not in MODIS and WRF-Chem, and thus equally weights event and non-event conditions. Since the Accuracy quantifies model skill in correctly identifying both extreme and non-extreme aerosol loadings, it is thus indicative of model performance in capturing the overall AOD spatial variability.”

Interpretation of the three metrics is also included in section 3.3 (first paragraph) and in the Table 6 caption.

p 27324, l 16: Why is this done for a single reference location only? Wouldn't it make more sense to use a reference location on the East coast where more pollution exists anyway?

We chose the center of WRF-Chem simulated domain as reference location for several reasons:

- 1) to be comparable to Sullivan et al. (2015) where it is also shown that moving the centroid did not greatly impact the coherence estimates**
- 2) to represent a grid cell that closely represents the center of gravity of the domain**

We added the following to support our choice:

“The reference location represents the center of gravity of the domain and was previously used by Sullivan et al. (2015) for assessing scales of coherence. In that work they also found the spatial scales of coherence are not sensitive to the precise choice of reference location.”

p 27325, l 5: Table 3 shows that largest non-zero MFB occurs when MODIS Terra is compared to AERONET AOT. Doesn't this suggest that either Terra is really wrong (and not suited to evaluate WRF) or AERONET is already unrepresentative for scales like the 10 km MODIS pixel (unlikely)?

Thanks for this comment. We clarified in the text and Table 3 that the MFB of MODIS vs. AERONET is strongly affected by some outlier sites and the MFB decreases when we remove the three most biased sites. Further, the number of co-samples between MODIS is quite limited, thus those MFB may be not very representative. We added the following comment:

“When MODIS is compared to the 22 AERONET stations the MFB is -1.23 suggesting an underestimation of AERONET relative to MODIS. The large bias can be explained noting that the number of co-samples between MODIS is quite small and that MFB is strongly impacted by a few outliers. When we remove the three most biased sites (one land site in the North and two sites along the East coast) the MFB decreases to -0.91.”

p 27326, l 6: "because WRF-Chem simulates high AOD and aerosol nitrate and sulfate concentrations". This is a sweeping statement with no evidence to support it. Please remove or elaborate.

We included more analyses on the chemical composition comparison and modified the text accordingly. Please see detailed response to reviewer 3.

p 27326, l 21: "occupy much of the same parameter space". This sentence is confusing. How can WRF-Chem comparisons with AERONET (M-O) be compared to AERONET or MODIS observations (O)?

The comparison between WRF-Chem and MODIS is done by gridding L2-MODIS data to 12km to match model grid, whereas comparison between WRF/MODIS and AERONET is done by comparing hours with simultaneous data in the grid cell including each AERONET station. We modified the manuscript accordingly in the data section as discussed before.

p 27326, l 23: "model simulations reproduce the range and probability of low uncertainty AERONET measured AOD nearly as well as MODIS." But the times and locations can be way off. It is important to comment on this aspect. EQQ plots can only take you so far.

We agree. The EQQ plots do not necessarily simultaneously compare the same MODIS-AERONET and WRF-Chem-AERONET pairs. We rephrased as follows:

“However, it is worthy of note that WRF-Chem comparisons with AERONET observations occupy much of the same observational range as simultaneous MODIS and AERONET at those sites (Fig. 9a), although the EQQ plot does not necessarily compare the same MODIS-AERONET and WRF-Chem-AERONET data pairs (i.e. the sample used to compare AERONET and MODIS may differ from that used to compare WRF-Chem and AERONET due to the cloud screening procedure).”

p 27326, l 27: "Nevertheless,". Why nevertheless? These correlations seem very low to me. Maybe that is due to observational error but I doubt it. AE MFB WRF-Chem AERONET = -0.59, so a substantial bias (note that AERONET AE have been averaged over 20 individual measurements during a month reducing measurement errors), so WRF-Chem probably has an issue in correctly simulating AE anyway.

We rephrased as follows:

Despite the low confidence in AE retrievals from MODIS, the comparison of WRF-Chem with the remote sensing estimates indicates some degree of agreement. The overall MFB of WRF-Chem vs MODIS Terra is -0.09 (-0.11 vs. Aqua) and the correlation between WRF-Chem and MODIS monthly mean AE seems to be independent of season and lies between 0.20 and 0.54 for all months except April, May and November when it is lower, whereas r is always < 0.14 when comparing with MISR (Fig. 7b).

p 27327, l 14: "After cloud screening". Why after cloud screening? I thought all model data used in comparison with observations are cloud-screened to start with?

Yes, it's correct. We removed "after cloud screening" to avoid confusion.

p 27328, l 12: the threshold for extreme AOT events (p75) is different for WRF-Chem and MODIS. How different is it?

Given we already focused on the quantification of the bias in AOD magnitude, now we are analysing differences in distribution and in spatial patterns. As an example, for Aqua, the p75 threshold varies by a minimum of 7% larger for WRF-Chem relative to MODIS in July to up a three times larger during the month of October when we already know the model has a larger bias in AOD due to the underestimation of precipitation.

p 27330, l 12: AOD=0.22 is a domain-average for clear grid-cells. So the orbit of MODIS was not taken into account? The MFB is thus calculated from two datasets with different spatial sampling? If so, that would be plain wrong.

No, we are still considering data over the same grid for hours of satellite overpass time. We rephrased for clarity as follows:

“After grid cells with any cloud presence are removed and considering only overpass hours, the domain averaged simulated mean AOD is 0.22.”

p 27330, l 18: AERONET MFB=0.5 according to Table 1

Thanks, fixed.

p 27330, l 22: Please also discuss/mention clear north-south gradient in AOT bias vs Terra (Fig 6). Maybe relative errors do not show a gradient? Does this gradient also exist in yearly precip errors (like Fig S3)?

The figure below shows that the N-S gradient is still present when we use NMB to evaluate model performance. We explicitly note this pattern in the text:

“A clear North-South gradient in AOD bias vs MODIS is also observed.”

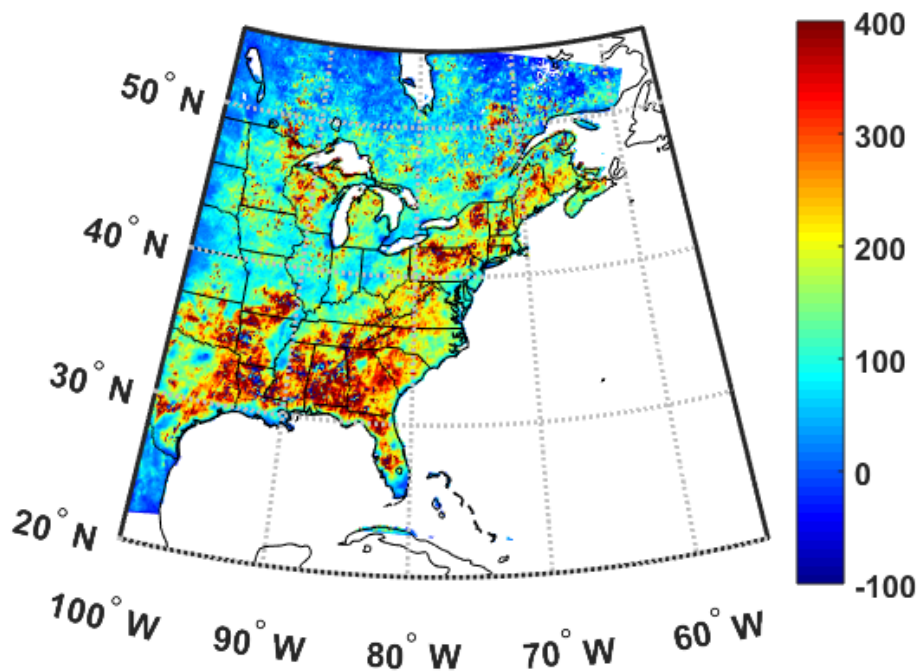


Figure. Normalized Mean Bias of AOD from WRF-Chem and Terra on a yearly basis.

p 27331, l 6: Table 3 suggests AE MFD vs AERONET is -0.59

Thanks, fixed.

p 27331, l 9: "the bias relative to AERONET is consistent with prior research (Table 1) and is symptomatic of relatively poor model performance for this metric." A non-zero bias is not symptomatic of poor model performance, it is one of the most important metrics by which we judge model performance.

We rephrased as follows:

“the large bias relative to AERONET is consistent with prior research (Table 1), and is symptomatic of substantial systematic error.”

p 27331, l 22: "central tendency" -> mean or average

Changed with “mean AOD values”.

p 27331, l 23: Not 'maximized' but 'greater'. After all, you talk about high loadings, not the highest loadings

Done

p 27348: Larger symbols for AERONET sites would be useful

We modified Figure 1 making larger symbols and including the MFB for AOD at AERONET locations (previously in Figure 2).

p 27349: Numbers in plot hard to read and not very useful anyway because exact location of site not clear and lot of fine structure in underlying MODIS data. Consider removing AERONET data.

We removed the numbers and included those relative to AOD in Figure 1 to save the information regarding the spatial variability in model performance.

p 27350: the lack of spatial variation in the observations is striking. Is this simply because of the colorbar scale? Or does WRF-Chem show more variation?

We remade the figure setting a different colorbar scale for WRF-Chem and EPA for easier visualization of the spatial variability in the observations.

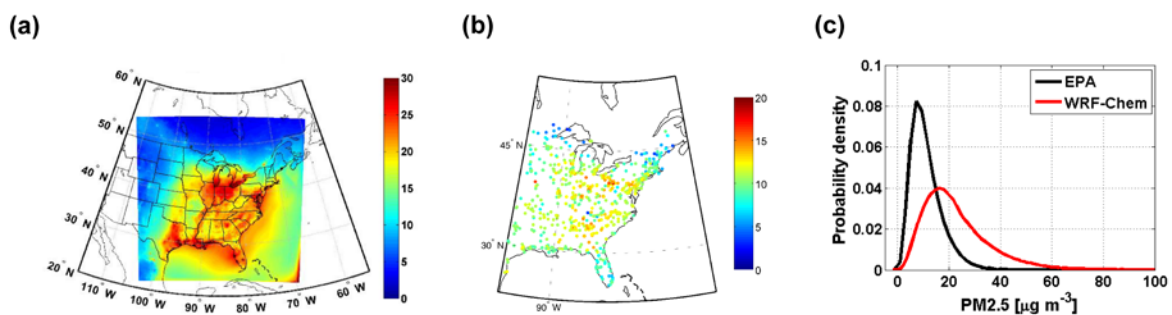


Figure 3. Mean daily PM_{2.5} concentrations [$\mu\text{g m}^{-3}$] during 2008 as (a) simulated by WRF-Chem in the layer closest to the surface and (b) observed at 1230 EPA sites (note the different colorbar). Panel (c) shows the probability distribution of daily mean PM_{2.5} concentrations observed (black line) and simulated (red line) at the measurement stations.

p 27351: While an interesting attempt at presenting a lot of information concisely, I find it difficult to easily separate the different coloured rings. Rather, one might try to use color (MFB, blue-red scale), symbol size (correlation) and symbol (RMSD, clearly this requires the RMSD to be binned in to 5 or so range bins) to denote the same information.

We remade this figure.

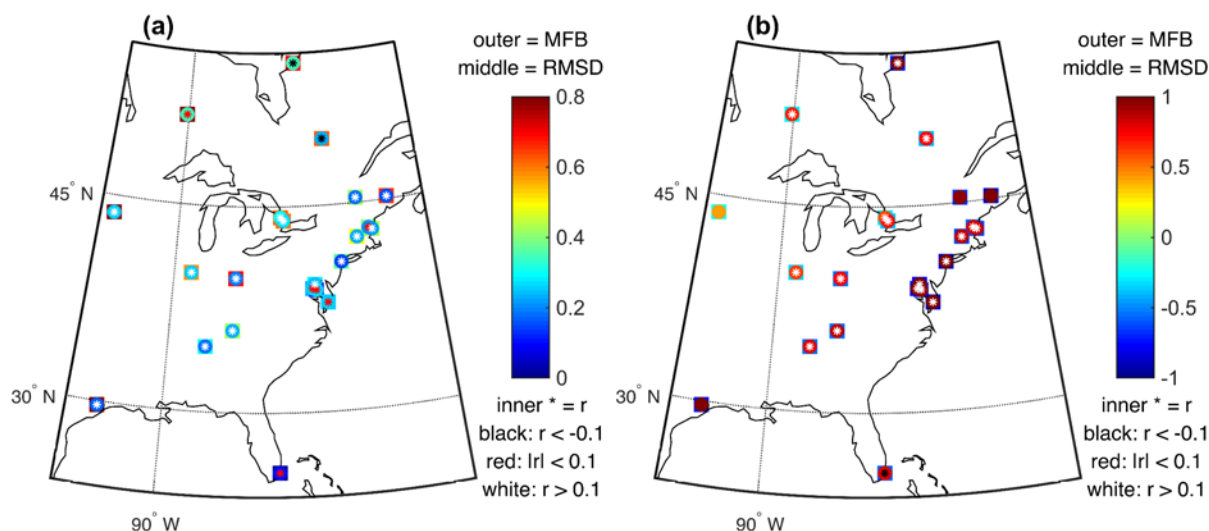


Figure 5. Summary statistics of comparisons of WRF-Chem simulations of (a) AOD and (b) AE relative to simultaneous observations at the AERONET sites. For a location to be included in this analysis at least 20 coincident observations and simulations must be available. The symbols at each AERONET station report MFB (outer square), root mean squared difference (RMSD, outer circle) and correlation coefficient (r , inner *). Note the different colorbar for MFB and RMSD between the two frames. The correlation coefficient is displayed with different colors according with 3 classes: $r < -0.1$ (black), $|r| < 0.1$ (red) and $r > 0.1$ (white).

p 27352: It would be very interesting to see if these Taylor plots change when data is spatially aggregated first, i.e. what if model+obs are averaged over 12, 24, 48, 96 km before Taylor plots are made?

We performed this analysis and included a figure in the Supplementary Materials. The text was changed as follows:

“We also examined the impact of spatial aggregation (at 12, 24, 36, 48, 72 and 96 km) on the seasonality of model performance. For AOD the spatial correlations are largest for most months when data are aggregated to a resolution of 24×24 km and the ratio of spatial standard deviation is also closer to 1 when AOD are spatially aggregated, possibly indicating that the spatial patterns simulated by WRF-Chem at a fine scale do not always match those observed by MODIS (Fig. 8). For AE both spatial correlations and ratio of standard deviations do not vary significantly when data are aggregated to a coarser resolution (Fig. S5).”

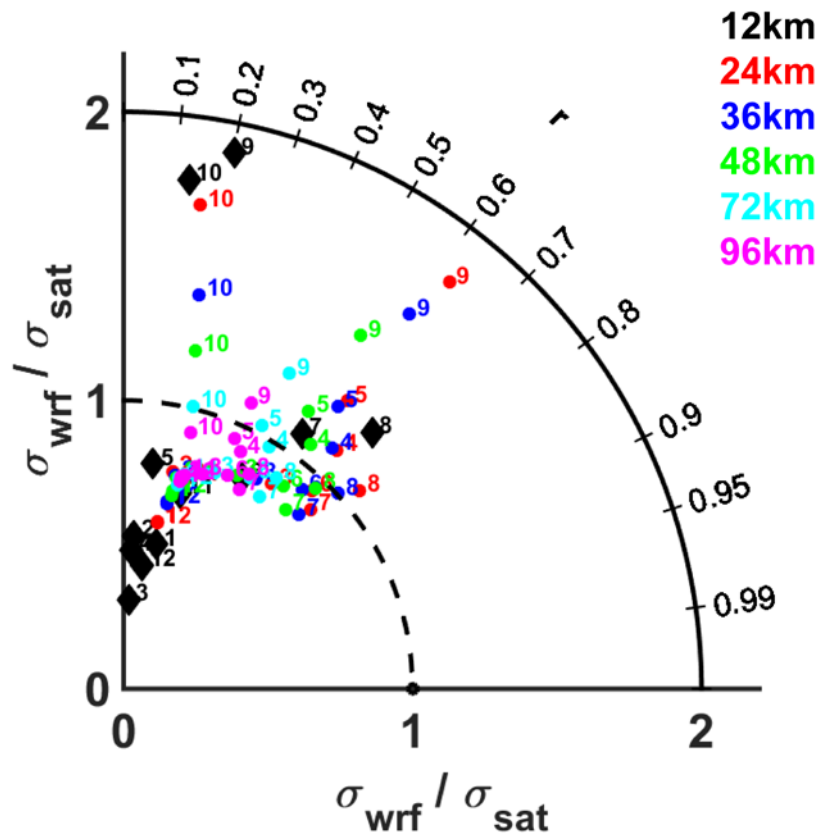


Figure 8. Taylor diagrams for AOD when MODIS observations and WRF-Chem simulations at 12 km are spatially aggregated to 24, 36, 48, 72 and 96 km. Numbers next to the colored dots/diamonds indicate different months.

Response to review comments on acp-2015-586 from reviewer 3

The original comments are provided in black, our response is given below each comment in red.

Thank you for the careful reading of our manuscript and your review.

This manuscript presents the evaluation of high-resolution WRF-Chem simulations over North America. The model skill in reconstructing the Aerosol Optical Depth and Angstrom Exponent is investigated by comparing model results with observations from MODIS Aqua and Terra as well as the ground networks AERONET and EPA. The research topic is certainly within the scope of the ACP. The article is well written and the methodology is clearly described. Moreover, aerosol optical properties are generally poorly constrained in modelling evaluation, especially at high-resolution resolution. For these reasons, I consider that such work should be published in ACP, but only after some revisions. It would have been worth to treat some aspects into more details, and to clarify some points of the discussion. I think that the authors should consider all the corrections of Anonymous Referee #2. In addition to his/her recommendations, I would propose some further corrections in the following.

Thank you for your positive assessment. We have indeed addressed all of the comments of the other reviewer.

General remarks:

- A major concern is that authors never make the connection to aerosol climate forcing, although the title suggests this kind of analysis. A thorough discussion on aerosol climate forcing is necessary. Otherwise the authors should modify the title.

We have modified the title to read:

“Evaluating the skill of high resolution WRF-Chem simulations in describing drivers of aerosol direct climate forcing at the regional scale”

- In many occasions, authors try to explain model biases in AOD estimations with an overestimation/underestimation of aerosol-nitrate and aerosol-sulfate, but no evidence are shown in the text to support this.

We thank the reviewer for raising this issue. In addition to the comparison of nitrate/sulfate ratios presented in the Supplementary Materials we added a further analyses using chemical composition data at 123 IMPROVE sites as explained further in the following points.

Technical corrections and comments:

Page 27316, line 9-14: This sentence is a bit confusing. Please restructure it.

We rephrased as follows:

Prior analyses of Level-3 (1° resolution) MODIS AOD over the eastern half of North America have indicated extreme AOD values (> local 90th percentile) are coherent over regional scales (~ 150 km) (Sullivan et al., 2015). Thus, our evaluation exercise also includes an analysis of the spatio-temporal coherence of extreme events.

Page 27322, line 3: Table 3 shows that MODIS and AERONET data are poorly correlated. In this section it is important to explain the reasons of this disagreement and the effects on the model evaluation.

Thanks for this comment. We clarified in the text and Table 3 that the MFB of MODIS vs. AERONET is strongly affected by some outlier sites and the MFB decreases when we

remove the three most biased sites. Further, the number of co-samples between MODIS is quite limited, thus those MFB may be not very representative. We added the following comment:

“When MODIS is compared to the 22 AERONET stations the MFB is -1.23 suggesting an underestimation of AERONET relative to MODIS. The large bias can be explained noting that the number of co-samples between MODIS is quite small and that MFB is strongly impacted by a few outliers. When we remove the three most biased sites (one land site in the North and two sites along the East coast) the MFB decreases to -0.91.”

Page 27323, line 9: What is i?

We changed the paragraph on χ^2 according to recommendation of reviewer 2.

Page 27325, line 6-9: Did your results suggest the same? Did you compare AOD biases with sulfate biases? Did you find a correlation between aerosol-sulfate and AOD estimations?

We added the following details in the Introduction:

“We also include intercomparison with daily mean PM_{2.5} concentrations from 1230 surface stations and near-surface PM_{2.5} composition using data from 123 IMPROVE sites. The PM_{2.5} concentration data for 2008 were obtained from the US Environmental Protection Agency (EPA) AirData web site and represent all available outdoor near-surface 24-hour mean PM_{2.5} measurements in the model domain. Most of these stations report values on a 1 day in 3 schedule. Daily average PM_{2.5} chemical composition are also available on 1 day in 3 and were accessed online through the IMPROVE data wizard.”

We added the following analysis and description in section 3.1:

“We further investigated the bias in PM_{2.5} by comparing WRF-Chem simulations with ground-based composition measurements at 123 IMPROVE sites in our domain. We computed the MFB on a seasonal basis between near-surface sulfate and nitrate concentrations in fine mode particles (i.e. Aitken and accumulation mode) (Fig. 4) and found sulfate concentrations are underestimated over almost the entire domain during winter, whereas a positive bias is present in the other seasons. Conversely, PM_{2.5} nitrate tends to be overestimated during winter and fall in the WRF-Chem simulations and underestimated during summer. Thus the positive bias in AOD and PM_{2.5} mass particularly during the summer appears to be associated with excess sulfate concentrations.”

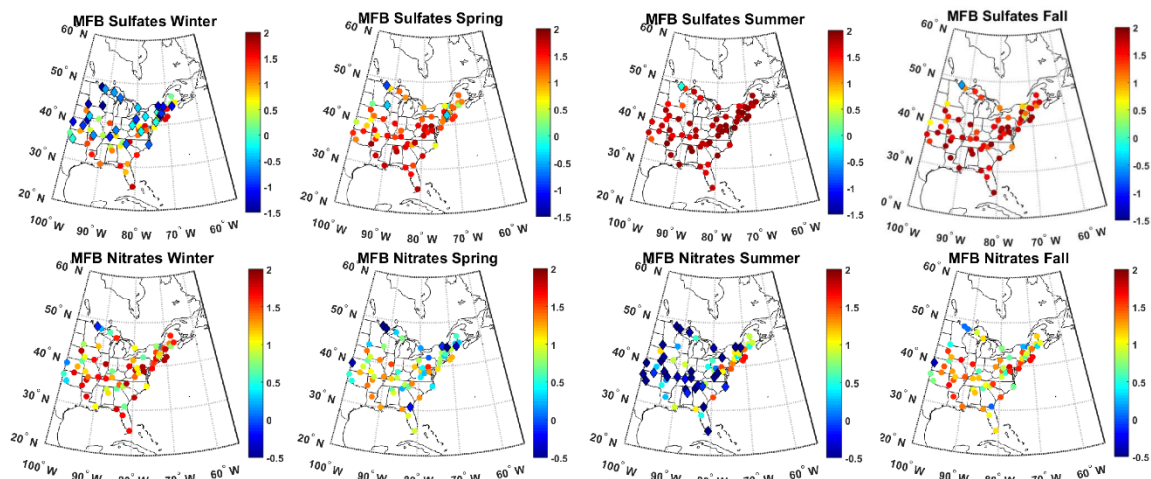


Figure 4. Mean fraction bias (MFB) of near-surface daily mean sulfate (first line) and nitrate (second line) concentrations in fine aerosol particles as simulated by WRF-Chem and observed in PM_{2.5} measurements at 123 IMPROVE sites in different seasons. A positive MFB indicates WRF-Chem overestimates the observations. Note the scales differ between the frames shown for sulfate and nitrate and dots/diamonds refer to positive/negative MFB.

Page 27326, line 5-8: Do you have evidence about this? You should support di statement with some elaborations.

Thanks for pointing this out. We added explicit reference to Figure S3 in the Supplementary Material and the new Figure 4 showing the MFB analysis.

Page 27329, line 17-23: One more time, you only did some hypothesis but no evidence to support these statements. Please, show some elaborations that include particle composition evaluation.

We added explicit references to the new analyses on composition discussed above.

Page 27329, line 23-24: Why higher uncertainties at coastlines? Do you have some previous studies to cite in order to support this?

We added the following reference to support our statement:

Anderson, J. C., Wang, J., Zeng, J., Leptoukh, G., Petrenko, M., Ichoku, C., and Hu, C.: Long-term statistical assessment of Aqua-MODIS aerosol optical depth over coastal regions: bias characteristics and uncertainty sources, Tellus Series B-Chemical and Physical Meteorology, 65, 10.3402/tellusb.v65i0.20805, 2013

Page 27330, line 18: Table 3 suggests that AERONET MFB is 0.5

Thanks, fixed.

Page 27331, line 6: AERONET MFB is -0.59 according to Table 3

Thanks, fixed.

1 Evaluating the skill of high resolution WRF-Chem
2 simulations in describing drivers of aerosol direct climate
3 forcing at the regional scale

4 ~~How skillfully can we simulate drivers of aerosol direct~~
5 ~~climate forcing at the regional scale?~~

6
7 **P. Crippa¹, R. C. Sullivan², A. Thota³, S. C. Pryor^{2,3}**

8 [1] COMET, School of Civil Engineering and Geosciences, Cassie Building, Newcastle
9 University, Newcastle upon Tyne, NE1 7RU, UK

10 [2] Department of Earth and Atmospheric Sciences, Bradfield Hall, 306 Tower Road, Cornell
11 University, Ithaca, NY 14853, USA

12 [3] Pervasive Technology Institute, Indiana University, Bloomington, IN 47405, USA

13 Correspondence to: P. Crippa (paola.crippa@ncl.ac.uk)

14
15 **Abstract**

16 Assessing the ability of global and regional models to describe aerosol optical properties is
17 essential to reducing uncertainty in aerosol direct radiative forcing in the contemporary climate
18 and to improving confidence in future projections. Here we evaluate the skill-performance of
19 high-resolution simulations conducted using the Weather Research and Forecasting model with
20 coupled chemistry (WRF-Chem) in capturing spatio-temporal variability of aerosol optical
21 depth (AOD) and Ångström exponent (AE) by comparison with ground- and space- based
22 remotely sensed observations. WRF-Chem is run over eastern North America at a resolution of
23 12 km for a representative year (2008). A ~~small~~-systematic positive bias in simulated AOD
24 relative to observations is found (annual MFB=0.175 and 0.50 when comparing with MODIS
25 and AERONET respectively), whereas the spatial variability is well captured during most
26 months. The spatial correlation of observed and simulated AOD shows a clear seasonal cycle
27 with highest correlation during summer months ($r=0.5-0.7$) when the aerosol loading is large

28 and more observations are available. ~~AE is retrieved with higher uncertainty from the remote~~
29 ~~sensing observations.~~ The model is biased towards simulation of coarse mode aerosols (annual
30 MFB for AE = -0.10 relative to MODIS and -0.59 for AERONET), but the spatial correlation
31 for AE with observations is 0.3-0.5 during most months, despite the fact that AE is retrieved
32 with higher uncertainty from the remote sensing observations. WRF-Chem also exhibits high
33 skill in identifying areas of extreme and non-extreme aerosol loading, and its ability to correctly
34 simulate the location and relative intensity of ~~an~~ extreme aerosol events (i.e. AOD>75th
35 percentile) varies between 30 and 70% during winter and summer months respectively.

36

37 1. Introduction and Objectives

38 Atmospheric aerosol particles (aerosols) play a major role in dictating Earth's climate by both
39 directly interacting with solar radiation (direct effect) and acting as cloud condensation nuclei
40 and thus changing cloud properties (indirect effect) (Boucher et al., 2013). The global mean
41 aerosol direct effect is estimated to be -0.27 (possible range of -0.77 to +0.23) W m⁻², while the
42 indirect effect is -0.55 (-1.33 to -0.06) W m⁻² (Stocker et al., 2013). Therefore their combined
43 radiative forcing is likely a significant fraction of the overall net anthropogenic climate forcing
44 since pre-industrial times (i.e. 1.13-3.33 W m⁻² (Stocker et al., 2013)) and a substantial source
45 of uncertainty in quantifying anthropogenic radiative forcing.

46 Accurate quantification of direct aerosol radiative forcing is strongly dependent on aerosol
47 precursor and primary aerosol emissions. Both have evolved over the past two decades in terms
48 of their spatio-temporal distribution and absolute magnitude. Emissions have generally
49 increased in emerging economies (Kurokawa et al., 2013), biogenic and anthropogenic
50 emissions have altered in response to changing land use and land cover (Wu et al., 2012), and
51 the implementation of pollution control strategies particularly in North America and Europe
52 have resulted in declines in air pollutant emissions (Xing et al., 2015; Giannouli et al., 2011).
53 Therefore there is evidence that aerosol burdens and thus direct climate forcing has varied
54 markedly in the past and may change substantially in the future. Further, although best estimates
55 of global anthropogenic radiative forcing from the aerosol direct and indirect effect are -0.27
56 and -0.55 W m⁻² (Stocker et al., 2013) respectively, the short residence time and high spatio-
57 temporal variability of aerosol populations mean their impact on regional climates can be much
58 larger than the global mean but are even more uncertain.

59 Long-term measurements of aerosol properties are largely confined to aerosol mass (total, PM₁₀
60 or PM_{2.5}) in the near-surface layer which may or may not be representative of either the total
61 atmospheric burden (Ford and Heald, 2013;Alston et al., 2012), or radiation extinction and
62 hence climate forcing. Further, aerosol composition measurements are often a 24-hour
63 integrated sample taken only 1 in 3 days and thus are subject to under sampling. Hence they
64 provide an incomplete description of temporal variability and mean aerosol burdens for model
65 performance evaluation. Long-term continuous and high-precision measurements of aerosol
66 properties are largely confined to aerosol mass (total, PM₁₀ or PM_{2.5}) in the near-surface layer
67 which may or may not be representative of either the total atmospheric burden (Ford and Heald,
68 2013;Alston et al., 2012), or radiation extinction and hence climate forcing. Columnar remote
69 sensing measurements of aerosol optical properties are available from a range of ground-based
70 and satellite-borne instrumentation, but have only a relatively short period of record, are subject
71 to non-zero measurement uncertainty (and bias), and under-sample the range of atmospheric
72 conditions due to cloud masking and infrequent satellite overpasses. Therefore, regional and
73 global models are most commonly used to quantify historical and contemporary aerosol direct
74 radiative forcing based on simulated properties such as the aerosol optical depth (AOD) and
75 Ångström exponent (AE) (Boucher et al., 2013).

76 Most global models that include aerosol microphysics have been run at fairly coarse resolution
77 (spatial resolution of the order of 1-2.5°) (Table 1) usually for periods of a few years. The
78 resulting fields of AOD (and less frequently AE) have been evaluated relative to ground-based
79 and satellite-borne remote sensing optical properties measurements (Table 1). However, aerosol
80 populations (and dynamics) are known to exhibit higher spatial variability (and scales) than can
81 be manifest in those models (Kovacs et al.,2006;Kulmala et al., 2011;Santese et al., 2007;
82 Schutgens et al., 2013;Sinzuka and Redemann, 2011). ~~However, aerosol populations (and~~
83 ~~dynamics) are known to exhibit higher spatial variability (and scales) than can be manifest in~~
84 ~~those models (Kulmala et al., 2011;Spracklen et al., 2010).~~ Despite recent improvements in the
85 sophistication of aerosol processes and properties within global models, there are still
86 substantial regional and latitudinal discrepancies in both the magnitude of AOD and other
87 aerosol properties which impact aerosol direct radiative forcing and the degree of model-to-
88 model agreement (Myhre et al., 2013). Thus the skill of these models in reproducing the spatio-
89 temporal variability in the aerosol size distribution, composition, concentration and radiative
90 properties is incompletely characterized. Further large model-to-model variability both in the
91 global mean direct aerosol forcing and in the spatial distribution thereof exists (Kulmala et al.,

92 ~~2011;Myhre et al., 2013) leading to high uncertainty in quantification of aerosol climate~~
93 ~~forcing. The skill of these models in reproducing the spatio-temporal variability in the aerosol~~
94 ~~size distribution, composition, concentration and radiative properties is incompletely~~
95 ~~characterized. Accordingly, there is large model to model variability both in the global mean~~
96 ~~direct aerosol forcing and in the spatial distribution thereof (Kulmala et al., 2011;Myhre et al.,~~
97 ~~2013).~~ Although a direct comparison between the studies summarized in Table 1 is inherently
98 very difficult due to the different performance metrics reported, and variations in both the model
99 resolution and aerosol descriptions, there is a consistent finding of high spatial variability in
100 model bias, both in sign and magnitude. Correlation coefficients of monthly and seasonal mean
101 AOD from model simulations versus satellite-based measurements are typically in a range ~0.6-
102 0.8 both in global (Colarco et al., 2010;Lee et al., 2015) and regional (Nabat et al., 2015)
103 simulations. However, these correlations are largely reflective of the ability of the models to
104 capture the seasonal cycle and columnar aerosol properties from remote sensing and thus ignore
105 substantial variability on the synoptic (Sullivan et al., 2015) and meso-scales (Anderson et al.,
106 2003). A wider range of correlation coefficients are reported when comparisons are made to
107 high frequency observations of AOD at the hourly/daily timescale both in global (Sič et al.,
108 2015) and regional (Rea et al., 2015) simulations ($r \sim 0.3-0.8$). The largest range of correlation
109 coefficients ($[-0.99, 0.9]$; Table 1) is reported when simulated AOD is compared with
110 observations from the AERosol RObotic NETwork (AERONET), and appear to be function of
111 temporal averaging, location of AERONET sites and model resolution. Correlations between
112 time series of simulated AE versus AERONET observations are reported less frequently, and
113 when conducted for monthly mean values range from ~0.4 (Li et al., 2015) to ~0.8 (Colarco et
114 al., 2010).

115 At least some of the variability in model skill performance, as indicated by the mutual variability
116 with observations described by correlation coefficients, and model-to-model agreement shown
117 in AeroCom Phase II may be attributable to variations in model resolution, differences in gas
118 and particle phase parameterizations and aerosol descriptions. However, there are also
119 variations in the way in which model skill is evaluated and divergent opinions regarding
120 prioritization of future research directions.~~However, there are also variations in the way in~~
121 ~~which model skill is evaluated leading to ambiguity in terms of prioritizing future research~~
122 ~~directions.~~ The direct effect remains poorly quantified at the regional scale, due to uncertainty
123 in aerosol loading, uncertainty and spatio-temporal variability in aerosol physical properties
124 (Colarco et al., 2014) and a relative paucity of rigorous model verification and validation

125 exercises. Confidence in projections of possible future aerosol radiative forcing requires
126 detailed assessment of skill in the current climate, and the need for and benefits of regional
127 downscaling and/or use of high-resolution global models requires careful quantification.

128 Regional models represent an opportunity to assess if running higher resolution simulations
129 over specific regions of interest improves the characterization of aerosol optical properties of
130 relevance to direct radiative forcing. Assessment of value added (or lack thereof) from high
131 resolution regional versus global coarse resolution models has not been clearly quantified in
132 previous studies (Table 1).~~Assessment of value added (or lack thereof) from high resolution~~
133 ~~regional versus global coarse resolution models is not quantifiable from prior studies alone.~~
134 Although high-resolution simulations, comparable to those presented herein, have been run,
135 they are over a small temporal and spatial domain (e.g. (Tuccella et al., 2015)), or lack
136 quantitative assessment of aerosol optical properties (e.g. (Tessum et al., 2014)). Thus,
137 quantification of the skill of high-resolution modeling of aerosol optical properties is presented
138 here along with a preliminary analysis of model performance as a function of spatial
139 aggregation. Forthcoming work will include direct comparison to coarser resolution
140 simulations to quantify the value added (or lack thereof) from increased model resolution.

141 We evaluate the skill of state-of-the-art high-resolution regional model simulations of climate-
142 relevant aerosol properties using a range of ~~inferential-descriptive~~ statistics and investigate
143 possible sources of discrepancies with observations. The impact of aerosols on climate and
144 human health are strengthened under conditions of enhanced aerosol concentrations, thus it is
145 necessary to study and diagnose causes of ‘extreme aerosol events’ (Chu, 2004;Gkikas et al.,
146 2012), and to evaluate the ability of numerical models to simulate their occurrence, intensity,
147 spatial extent and location. Prior analyses of Level-3 (1° resolution) MODIS AOD over the
148 eastern half of North America have indicated ~~the frequency of co-occurrence of~~ extreme AOD
149 values (> local 90th percentile) are coherent over decreases to below 50% at regional scales (~
150 150 km) from a central grid cell located in southern Indiana, but is above that expected by
151 ~~random chance over almost all of eastern North America~~ (Sullivan et al., 2015). Thus, our
152 evaluation exercise also includes an analysis of the spatio-temporal coherence of extreme
153 events.

154 We applied the Weather Research and Forecasting model with coupled Chemistry (WRF-Chem
155 version 3.6.1) at high resolution (12×12 km) over eastern North America during the year 2008,
156 in the context of a pseudo type-2 downscaling exercise in which the high-resolution model is

157 nested within reanalysis boundary conditions (Castro et al., 2005). The choice of this spatial
158 resolution is taken in part to match the resolution of North American Mesoscale Model that is
159 used for the meteorological lateral boundary conditions and to ensure we capture some
160 mesoscale variability while remaining computationally feasible.

161 Our evaluation is designed to investigate spatio-temporal variability of aerosol optical
162 properties (i.e. AOD and AE) in their mean and extreme values. Thus, we conduct our
163 evaluation of the simulations using:

- 164 (i) High-frequency, disjunct time series data from ~~columnar~~ point measurements at
165 AERONET stations.
- 166 (ii) Relatively high-resolution spatial data from lower frequency (once daily or lower)
167 data from polar orbiting satellites (i.e. MODIS and MISR).

168 We also include intercomparison with daily mean PM_{2.5} concentrations from 1230 surface
169 stations and near-surface PM_{2.5} composition using data from 123 IMPROVE sites. The PM_{2.5}
170 concentrations ~~se~~-data for 2008 were obtained from the US Environmental Protection Agency
171 (EPA) AirData web site and represent all available outdoor near-surface 24-hour mean PM_{2.5}
172 measurements in the model domain. Most of these stations report values on a 1 day in 3
173 schedule.- Daily average PM_{2.5} chemical compositions are also available on 1 day in 3 and were
174 accessed online through the IMPROVE data wizard. We further evaluate the WRF-Chem
175 simulations of a key meteorological parameter – precipitation – relative to observations from
176 the Delaware gridded dataset (Matsuura and Willmott, 2009). This data set includes monthly
177 accumulated precipitation data on a 0.5×0.5° grid which is estimated by interpolating station
178 observations from the Global Historical Climatology Network using the spherical version of
179 Shepard's distance-weighting method (Shepard, 1968; Willmott et al., 1985).

180 This paper is structured as follows. We first describe the settings used in our WRF-Chem
181 simulations and introduce the remote sensing and other data used for model evaluation (Sect.
182 2). A description of statistical metrics used for the evaluation is also provided. Section 3
183 presents results of the evaluation of simulated AOD and AE versus observations, as well as
184 findings on extreme AOD values. In Section 4 we summarize our findings and draw
185 conclusions.

186 **2. Methods**

187 **2.1 WRF-Chem simulations**

188 The Weather Research and Forecasting Model with coupled chemistry (WRF-Chem, version
189 3.6.1) (Grell et al., 2005;Fast et al., 2006) is used to simulate aerosol processes over eastern
190 North America during the whole of 2008. The simulation domain comprises 300×300 grid
191 points with 12 km resolution and is centered in southern Indiana (86°W, 39°N). The calendar
192 year 2008 was selected because it is representative of average climate and aerosol conditions
193 in the center of the model domain (near Indianapolis, IN). In 2008, mean T_{\max} , T_{\min} ,
194 precipitation, and wind speed as measured at the National Weather Service Automated Surface
195 Observing Systems (NWS ASOS) station at Indianapolis International Airport are within ± 0.25
196 standard deviations (σ) of the 2000-2013 seasonal means. Further, mean seasonal AOD from
197 Level-3 MODIS retrievals is within $\pm 0.2\sigma$ of 2000-2013 mean values. Additionally, choice of
198 this year ensures availability of multiple sources of ground- and space-based measurements of
199 aerosol properties for evaluation of the simulations.

200 Table 2 provides details of the WRF-Chem simulations. In brief, we used 32 vertical levels up
201 to 50 hPa with telescoping to allow for a good vertical resolution in the boundary layer (i.e.
202 approximately 10 layers below 1 km for non-mountainous regions). Meteorological lateral
203 boundary conditions are provided every 6 hours from the North American Mesoscale Model
204 (NAM) applied at 12 km resolution. The initial and boundary chemical conditions are based on
205 output from the offline global chemical transport model MOZART-4 (Model for Ozone and
206 Related chemical Tracers, version 4), driven by meteorology from NCEP/NCAR-reanalysis
207 (Pfister et al., 2011;Emmons et al., 2010). Anthropogenic emissions are from the POET
208 (Precursors of Ozone and their Effects in the Troposphere) and the EDGAR (Emissions
209 Database for Global Atmospheric Research) databases. The land cover is specified based on
210 the USGS 24-category data at 3.7 km resolution (Anderson et al., 1976). Anthropogenic point
211 and area emissions at 4 km resolution are input hourly from the U.S. National Emissions
212 Inventory (NEI-05) (US-EPA, 2009) and specified for 19 vertical levels (see Fig. 1 for an
213 overview of the primary aerosol emissions). Biogenic emissions of isoprene, monoterpenes,
214 other biogenic VOC (OVOC), and nitrogen gas emissions from the soil are described as a
215 function of simulated temperature and photosynthetic active radiation (for isoprene) using the
216 model of Guenther (Guenther et al., 1993;Guenther et al., 1994;Simpson et al., 1995). Aerosol
217 and gas phase chemistry are described using the second generation Regional Acid Deposition

218 Model (RADM2) chemical mechanism (Stockwell et al., 1990) and the Modal Aerosol
 219 Dynamics Model for Europe (MADE) which incorporates the Secondary Organic Aerosol
 220 Model (SORGAM) (Ackermann et al., 1998;Schell et al., 2001). The correct characterization
 221 of aerosol optical properties is ~~strongly related to~~dependent on model skill in describing particle
 222 composition and mixing state (Li et al., 2015;Curci et al., 2014). With this in mind, it is worthy
 223 of note that aerosol components are assumed to be internally mixed within each mode (although
 224 the composition differs by mode). ~~For the~~The standard deviation on the log-normal Aitken and
 225 accumulation modes the ~~median diameters are 10 nm and 70 nm with~~ standard deviations ~~of~~
 226 are fixed at 1.6 and 2, respectively. The choice of a modal representation of aerosol size
 227 distribution is dictated by the high computational demand of more sophisticated approaches
 228 (e.g. sectional description of the aerosol size distribution) for long-term simulations. With the
 229 current settings, the 1-year run was completed without restart in 9.5 days (230 hours) on the
 230 Cray XE6/XK7 supercomputer (Big Red II) owned by Indiana University using 256 processors
 231 distributed on 8 nodes, thus indicating feasibility of this configuration for climate scale
 232 simulations. Aerosol, and gas phase concentrations and meteorological properties are saved
 233 once hourly. AE from the WRF-Chem simulations is computed using:

$$234 \quad AE = \frac{\ln \frac{AOD_{400nm}}{AOD_{600nm}}}{\ln \frac{600nm}{400nm}} \quad \text{_____} (1).$$

235 AOD at wavelengths (λ) of 500 and 550 nm for comparison with MODIS and MISR
 236 respectively, are derived using the Ångström power law:

$$237 \quad AOD_{\lambda} = AOD_{300} \times \frac{\lambda^{(-AE)}}{300} \quad \text{_____} (2).$$

238 We investigated the wavelength dependence on AE calculation using λ at 300 nm and 1000 nm
 239 as proposed in (Kumar et al., 2014) and found that, although AOD estimates are independent
 240 on the wavelength range selected, $AE_{400-600nm}$ is systematically lower than $AE_{300-1000nm}$.
 241 Analyses of AE reported in this study are obtained using ~~$\lambda =$~~ wavelengths at 400 and 600 nm
 242 since they are closer to those used in AE satellite retrievals.

243 **2.2 Remotely-sensed data**

244 Consistent with previous research (Sect. 1 and Table 1), we evaluate the WRF-Chem
 245 simulations using four primary remote sensing products – three are drawn from instruments on

246 the Aqua and Terra satellites, while the fourth is from ground-based radiometers operated as
247 part of the AERONET network. The data sets are as follows:

248. The MODerate resolution Imaging Spectroradiometer (MODIS) instruments aboard the
249 polar-orbiting Terra (~1030 overpass local solar time (LST)) and Aqua (~1330 LST)
250 satellites. They have measured atmospheric aerosol optical properties since 2000 and 2002
251 respectively, with near-global daily coverage (Remer et al., 2005). Herein we use the Level
252 2 (L2; 10 km resolution) “dark-target” products of AOD at 550 nm and AE from 470 – 660
253 nm (Collection 5.1; (Levy et al., 2010)). The L2 AOD uncertainty is $\pm 0.05 \pm 0.15 \times \text{AOD}$
254 over land relative to global sun photometer measurements from AERONET; even when no
255 spatiotemporal averaging is used in the comparison (i.e. all combinations of MODIS
256 retrievals within 30 km of an AERONET site and all AERONET retrievals within 30 min of
257 the satellite overpass), 71% of MODIS retrievals fall within a $\pm 0.05 \pm 0.2 \times \text{AOD}$ envelope
258 relative to AERONET over E. CONUS (Hyer et al., 2011). ~~The L2 AOD uncertainty is \pm~~
259 ~~$0.05 \pm 0.15 \times \text{AOD}$ over land relative to global sun photometer measurements from~~
260 ~~AERONET.~~ AE is retrieved with higher uncertainty, and tends to exhibit a bi-modality in
261 retrieved values (Levy et al., 2010; Remer et al., 2005) (see ~~SM~~ Fig. S1). For this reason
262 where we compare WRF-Chem simulated AE with values from MODIS we treat AE as a
263 binary variable, wherein $\text{AE} < 1$ is taken as representing coarse mode dominated aerosol
264 populations and $\text{AE} > 1$ indicates fine mode dominated populations (Pereira et al.,
265 2011; Valenzuela et al., 2014).

266 2. The Multi-angle Imaging Spectroradiometer (MISR) instrument is also aboard the Terra
267 satellite, and measures radiances at four wavelengths from 446 – 886 nm at nine viewing
268 angles from nadir to 70.5° . MISR (L2, 17.6 km resolution) retrieves AOD with lower
269 uncertainty than MODIS ($\pm 0.05 \times \text{AOD}$ relative to AERONET), but with lower temporal
270 resolution (global coverage in ~ one week) (Kahn et al., 2010; Kahn et al., 2005). Herein, we
271 use the $0.5^\circ \times 0.5^\circ$ gridded Level 3 (Ver. 31) AOD (at 555 nm) and AE (calculated from
272 AOD at 443 and 670 nm).

273 3. Ground-based sun-photometer measurements from 22 AErosol RObotic NETwork
274 (AERONET) (Holben et al., 1998) stations are also used in this study (Fig. 1). This network
275 is highly spatially inhomogeneous, but under cloud-free conditions the observations are
276 available at multiple times during daylight hours. AOD is measured directly by the
277 AERONET sun photometers at seven wavelengths (340, 380, 440, 500, 670, 870, and

278 1020 nm) with high accuracy (i.e. AOD uncertainty of < 0.01 for $\lambda > 440$ nm (Holben et
279 al., 2001)). The Ångström Exponent (AE) is calculated for all available wavelengths within
280 the AOD range. The AE 870-440 nm includes the 870, 670, 500 and 440 nm AOD data.
281 Level-2 aerosol products from AERONET (i.e. cloud screened and quality assured) have
282 been used extensively in satellite and model validation studies (including many of those
283 summarized in Table 1) and are used herein.

284 To avoid the discontinuity in the MODIS retrieval algorithm due to different assumed aerosol
285 types (Levy et al., 2007), we confine our analyses of model skill to longitudes east of 98°W.
286 Only WRF grid cells with cloud fraction = 0 during the satellite over pass of each grid cell are
287 used in comparison to MODIS/MISR observations, and only grid cells with at least 5 valid
288 observations (both from MODIS/MISR and cloud-screened WRF) during a given month are
289 included in the analyses presented herein. ~~To avoid the discontinuity in the MODIS retrieval~~
290 ~~algorithm due to different assumed aerosol types (Levy et al., 2007), we confine our analyses~~
291 ~~of model skill to longitudes east of 98°W. All comparisons of modeled aerosol optical~~
292 ~~properties relative to MODIS observations (e.g. monthly mean values) only include grid cells~~
293 ~~for which at least 5 valid coincident observations are available during a given month after~~
294 ~~applying a cloud screen for overpass hours with cloud fraction larger than zero.~~ It is worth
295 noting that setting a threshold of 10 observations does not significantly affect the results. For a
296 uniform assessment, L2 MODIS and L3 MISR data have been interpolated from their native
297 grids (and resolutions of 10 km and $0.5^\circ \times 0.5^\circ$, respectively) to the WRF-Chem 12 km resolution
298 grid by computing the mean of pixels with valid data within 0.1°/0.3° for MODIS/MISR from
299 the model centroids ~~0.1° (-20 km) from the model centroids~~. The choice of averaging over a
300 slightly larger area than model resolution is dictated by the sparsity of valid ~~MODIS satellite~~
301 retrievals. For AERONET vs. MODIS comparison, we only use the nearest MODIS data (after
302 regridding to WRF) to each site. Where hourly WRF-Chem output is compared with data from
303 AERONET ~~stations~~ sites, a station is only included if there are at least 20 simultaneous estimates
304 available, and each AERONET measurement is compared to the nearest WRF-Chem time step
305 and to the grid cell containing the station.

306 **2.3 Statistical methods used in the model evaluation**

307 The primary error metric of overall model performance used herein is the Mean Fractional Bias
308 (Boylan and Russell, 2006):

$$MFB = \frac{1}{N} \sum_1^N \frac{C_m - C_0}{\frac{C_m + C_0}{2}} \quad (3).$$

310 MFB is a useful model performance indicator since it equally weights positive and negative
 311 biases. It varies between +2 and -2 and has a value of zero for an ideal model. Where MFB is
 312 reported for WRF-Chem versus MODIS-~~or~~/ MISR/AERONET, C_m is the monthly mean AOD
 313 or AE simulated by WRF-Chem at a specific location, C_0 refers to the same quantify from
 314 MODIS-~~or~~ MISR remote sensing data (Table 3) and N is the sample size. ~~Where MFB is~~
 315 ~~reported in comparisons of WRF-Chem with AERONET, the monthly average in the model~~
 316 ~~grid cell containing the AERONET site is compared with monthly averaged observations (C_0).~~

317 The evaluation of WRF-Chem simulations of AOD and AE relative to satellite retrievals
 318 (MODIS and MISR) is also summarized using Taylor diagrams (Taylor, 2001) produced from
 319 the monthly means for the grid cells with simultaneous data availability. Taylor diagrams
 320 synthesize three aspects of model skill focused on evaluations of the spatial fields of the
 321 parameter of interest. The correlation coefficient of the modeled vs. observed field which is
 322 expressed by the azimuthal position, the root mean squared difference which is proportional to
 323 the distance between a point and the reference point on the x-axis (at 1, 0), and the ratio of
 324 simulated and observed spatial standard deviation which is proportional to the radial distance
 325 from the origin.

326 To investigate model performance at given locations through time, empirical quantile-quantile
 327 (EQQ) plots are constructed using high frequency realizations of AOD and AE at individual
 328 locations (AERONET sites) relative to WRF-Chem values simulated in the grid cell containing
 329 the measurement site. EQQ plots are thus generated for each of the AERONET stations using
 330 all hours when there are simultaneous estimates available from the direct observations and from
 331 the numerical simulations. The advantage of EQQ plots is that they make no assumptions
 332 regarding the underlying form of the data, and can be readily used to determine which parts of
 333 the modeled distribution deviate from the observations (and thus fall away from a 1:1 line).

334 The validity of AE estimates is a function of both the absolute magnitude of AOD and the
 335 uncertainty in the wavelength dependent AOD. AE provides information regarding the relative
 336 abundance of fine to coarse particles. Thus, here we quantify the model skill in reproducing
 337 spatial patterns of fine and coarse mode particles observed by MODIS (Terra) by comparing
 338 the frequency distribution of AE lower and higher than 1 to distinguish populations dominated

339 by coarse and fine aerosols respectively in WRF-Chem and MODIS (Valenzuela et al.,
 340 2014;Pereira et al., 2011). The choice of this threshold reflects the AE distribution. AE
 341 simulated by WRF-Chem generally conforms to a single normal distribution centered on 1
 342 during January-April and on 1.3 from May-June to December; AERONET time series also tend
 343 to conform to a single mode, while MODIS estimates typically are bimodally distributed (see
 344 ~~SM-Fig. S1). A χ^2 -test is applied to assess if the frequency distribution of fine and coarse~~
 345 ~~partieles is the same between MODIS and WRF-Chem.~~ We therefore consider the data in the
 346 form of a contingency table (Table 4) and compute ~~the a χ^2 -test to assess if the frequency~~
 347 ~~distribution of fine and coarse particles is the same between MODIS and WRF-Chem. The χ^2~~
 348 ~~statistic is applied with~~ ~~with~~ one degree of freedom ~~from:~~

$$\chi^2 = \sum_{i=1}^N \frac{(O_i - E_i)^2}{E_i} \quad (4)$$

349 ~~where O_i is the frequency of observations of type i and E_i is the expected frequency of type i~~
 350 ~~which is computed as the product of the row total with the column total, divided by the total~~
 351 ~~number of observations. Herein we apply and aa 99% confidence limit to assess significance of~~
 352 ~~the χ^2 statistic.~~

354 As described above, the impact of aerosols on climate and human health are strengthened under
 355 conditions of enhanced aerosol concentrations, thus two analyses were undertaken to evaluate
 356 the ability of the WRF-Chem simulations to represent extreme AOD values:

- 357 1. Evaluation of the spatial patterns of extreme events. Using daily estimates of AOD in
 358 each grid cell and month we identified the 75th percentile value across space (i.e. $p75$)
 359 as threshold for extreme AOD for WRF-Chem and MODIS separately. Grid cells with
 360 AOD exceeding that threshold were classified as exhibiting extreme values. The
 361 consistency in the spatial distribution of extreme values as simulated by WRF-Chem
 362 relative to MODIS are quantified using three skill statistics: the Accuracy, Hit Rate (HR)
 363 and Threat Score (TS) defined in equations 5-74-6. In these equations, WE , ME , WN
 364 and MN correspond to ~~occurrence frequency~~ of extreme conditions in WRF-Chem (WE)
 365 or MODIS (ME) or not (WN or MN):

$$Accuracy = \frac{WE / ME + WN / MN}{WE / ME + WE / MN + WN / ME + WN / MN} \quad (54)$$

$$HR = \frac{WE / ME}{WE / ME + WN / ME} \quad (65)$$

$$TS = \frac{WE / ME}{WE / ME + WE / MN + WN / ME} \quad (76)$$

The Accuracy describes the fraction of grid cells co-identified as exceeding $p75$ or not in MODIS and WRF-Chem, and thus equally weights event and non-event conditions. Since the Accuracy quantifies model skill in correctly identifying both extreme and non-extreme aerosol loadings, it is thus indicative of model performance in capturing the overall AOD spatial variability. In this application, where extreme is identified as the 75th percentile, a value of 0.5 would indicate none of the grid cells experiencing extreme events were reproduced by the model, while 1 would indicate perfect identification of events and non-events. The HR and TS metrics give ‘credit’ only those grid cells identified as ‘extreme’. For these metrics, a value of 0 indicates no correct identification of grid cells with extreme values, while a perfect model would exhibit a value of 1.

2. Evaluation of the scales of coherence of extreme AOD. For each day during the overpass time and hours of clear sky conditions, we determine if AOD simulated at our reference location (i.e. the center of the domain, in Southern Indiana) is equal or larger than the local $p75$ for that grid cell and season and then identify all grid cells in the domain that also satisfy the condition of $AOD \geq \text{local } p75$. The reference location represents the center of gravity of the domain and was previously used by Sullivan et al. (2015) for assessing scales of coherence. In that work they also found the spatial scales of coherence are not sensitive to the precise choice of reference location. For each season, we thus compute the probability of extreme AOD co-occurrence at our reference site and any other grid cell as the frequency of co-occurrence divided by the number of extreme occurrences at the reference location. The spatial scales of extreme AOD are then estimated by binning the radial distance of each grid cell centroid from the domain center into 100 km distance classes. An analogous procedure is applied to L2 MODIS data to compare with simulations.

3. Results

3.1 Evaluation of AOD

Overall WRF-Chem is positively biased relative to remotely-sensed AOD. The spatial MFB is 0.1520 (0.14) when computed using all available MODIS measurements from Terra (Aqua)

397 and 0.50 relative to data from the AERONET stations (Table 3). The sign of this bias is
398 consistent across the entire simulation domain (Fig. 2). These results agree with findings from
399 previous regional studies that have also shown an overestimation of AOD by WRF-Chem over
400 eastern North America and Europe (i.e. regions dominated by sulfate aerosols), and
401 underestimation in western US and most of the rest of the globe (Zhang et al., 2012; Colarco et
402 al., 2010; Curci et al., 2014) (Table 1). Higher biases of WRF-Chem simulated annual mean
403 AOD are found in the southern portion of the domain (Fig. 2) where the model also exhibits a
404 positive bias in daily mean near-surface PM_{2.5} relative to observations from 1230 US EPA sites
405 (see Fig. 3 and SM-Fig. S2). We further investigated the bias in PM_{2.5} by comparing WRF-
406 Chem simulations with ground-based measurements of particle composition at 123 IMPROVE
407 sites over our domain. We computed the MFB on a seasonal basis between sulfate and nitrate
408 concentrations in fine mode particles (i.e. Aitken and accumulation mode) versus observations
409 (Fig. 4) and found sulfate concentrations are underestimated almost over the entire domain
410 during winter, whereas a positive bias is present in the other seasons. Conversely, nitrates tend
411 to be overestimated during winter and fall at most sites, whereas they are underestimated during
412 summer. Thus the positive bias in AOD and PM_{2.5} mass particularly during the summer appears
413 to be associated with excess sulfate concentrations.

414 The MFB of WRF-Chem relative to MODIS estimates of AOD is lower than the MFB relative
415 to most of the AERONET stations except for a few sites located along the coast, one polluted
416 site in the northeast and a few land sites in the North/North-West (Fig. 2e-1 and 45a). This is
417 possibly a result of an inability of the model to capture variations in aerosol optical properties
418 occurring at a local scale (below the resolution of 12 km). However, the evaluation statistics
419 for WRF-Chem relative to AERONET did not vary consistently with the classification of
420 AERONET stations. Indeed, the mean MFB for AOD in coastal, polluted and land sites varies
421 between 0.26 (coastal) and 0.67 (land), whereas for AE it varies between -0.72 (coastal) and -
422 0.50 (land). When MODIS is compared to the 22 AERONET stations the MFB is -1.23
423 suggesting an underestimation of AOD from AERONET relative to MODIS. The large bias can
424 be explained noting that the number of co-samples between MODIS is quite small and that
425 MFB is strongly impacted by a few outliers. When we remove the three most biased sites (one
426 land site in the North and two sites along the East coast) the MFB decreases to -0.91.
427 Using very limited data, prior research indicated mesoscale variability (horizontal scales of 40–
428 400 km and temporal scales of 2–48 h) is a common and perhaps universal feature of lower-
429 tropospheric aerosol light extinction [Anderson et al., 2003]. However, we are not aware of

430 prior systematic attempts to quantify and test the universality of AOD scales of coherence over
431 the contiguous US. To test the sensitivity of the MFB in simulated AOD to spatial aggregation,
432 we excluded the first 12 cells to the left and to the top of the simulated domain and averaged
433 the remaining 12×12 km grid cells over the following scales: 24×24, 36×36, 48×48, 72×72,
434 96×96, 144×144, 192×192, 216×216, 288×288, 384×384, 432×432, 576×576, 864×864,
435 1152×1152, 1728×1728, 3456×3456 km. The last spatial average corresponds to a single grid
436 cell encompassing the entire domain (excluding the outer 12 cells located to the West and North
437 of the simulation domain). Each spatial average at a coarser resolution is computed as the mean
438 of all valid 12×12 km grid cells within the averaging area. We then computed the MFB for the
439 regridded WRF-Chem and MODIS data pair and found that, on a yearly basis, MFB is highest
440 at 12km (0.14 for Aqua and 0.15 for Terra) and reaches a first minimum at 72 km for Aqua
441 (MFB=0.13) and 384 km for Terra (MFB=0.13) (see Fig. 6). However, the MFB and hence
442 systematic error in AOD relative to MODIS exhibits only a weak dependence on the level of
443 spatial aggregation.

444 Spatial patterns of monthly mean AOD show largest differences relative to MODIS during
445 winter months in the southern states and near the coastlines, which show MFB up to 0.7, and
446 lower spatial correlation (see Fig. 5a7a). This may be due to the larger uncertainty in MODIS
447 retrievals near the coast (Anderson et al., 2013), the smaller sample size in the observations
448 (particularly at high latitudes) during December to March or the lower overall AOD.
449 Conversely, the spatial correlation is maximized ~~over~~ during the summer (r=0.5-0.7) for
450 MODIS and August for MISR, when most data are available. The spatial variability of monthly
451 mean AOD fields is also well simulated by WRF-Chem during the warm season (months May-
452 August), as indicated by the ratio of the spatial standard deviation which is close to 1. However,
453 $\sigma(\text{AOD})$ ~~it~~ is usually higher in MODIS and/or MISR than in WRF-Chem. The RMSD is largest
454 and the spatial correlation is lowest during September and October, when MFB is also > 0.4 in
455 part because WRF-Chem simulates high AOD and aerosol nitrate and sulfate concentrations
456 over large regions in eastern North America (Fig. S3 and Fig. 4). The high positive bias in these
457 months is also reflected in the near-surface PM_{2.5} concentrations and its composition (SM-Fig.
458 S2 and Fig. 4). A possible explanation for the relatively poor model performance during
459 September and October may derive from the simulation of precipitation. During the majority
460 of calendar months, domain averaged precipitation as simulated by WRF-Chem is slightly
461 positively biased relative to the gridded observational data. However, during September and
462 October, the model exhibits a negative bias (of 8-10% relative to observations) and substantial

463 underestimation of precipitation in regions of typically high AOD such as the Ohio River valley
464 and along the east coast (SM Fig. 3S4). We also examined the impact of spatial aggregation
465 (at 12, 24, 36, 48, 72 and 96 km resolution) on the seasonality of model performance. For AOD
466 the spatial correlations are largest for most months when data are aggregated to a resolution of
467 24×24 km and the ratio of spatial standard deviation is also closer to 1 when AOD are spatially
468 aggregated, possibly indicating that the spatial patterns simulated by WRF-Chem at a fine scale
469 do not always match those observed by MODIS (Fig. 8). For AE both spatial correlations and
470 ratio of standard deviations do not vary significantly when data are aggregated to a coarser
471 resolution (Fig. S5).

472 Empirical quantile-quantile plots of AOD at AERONET stations computed for both
473 simultaneous MODIS observations and WRF-Chem with AERONET observations indicate that
474 the positive bias in WRF-Chem simulated values of AOD is evident across much of the
475 probability distribution (5th to 95th percentile values) at most AERONET stations. However, it
476 is worthy of note that WRF-Chem comparisons with AERONET observations occupy much of
477 the same observational range as simultaneous MODIS and AERONET at those sites (Fig. 9a),
478 although the EQQ plot does not necessarily compare the same MODIS-AERONET and WRF-
479 Chem-AERONET data pairs (i.e. the sample used to compare AERONET and MODIS may
480 differ from that used to compare WRF-Chem and AERONET due to the cloud screening
481 procedure) same parameter space as simultaneous MODIS and AERONET observations at
482 those sites (Fig. 6a). Thus, model simulations reproduce the range and probability of low-
483 uncertainty AERONET measured AOD nearly as well as MODIS.

484 3.2 Evaluation of AE

485 Despite the low confidence in AE retrievals from MODIS, the comparison of WRF-Chem with
486 the remote sensing estimates indicates some degree of agreement. The overall MFB of WRF-
487 Chem vs MODIS Terra is -0.09 (-0.11 vs. Aqua) and the correlation between WRF-Chem and
488 MODIS monthly mean AE seems to be independent of season and lies between 0.20 and 0.54
489 for all months except April, May and November when it is lower, whereas r is always < 0.14
490 when comparing with MISR (Fig. 7b). ~~As described above, AE is retrieved with much lower~~
491 ~~confidence than AOD from the MODIS measurements. Nevertheless, the correlation between~~
492 ~~WRF-Chem and MODIS monthly mean AE seems to be independent of season and lies between~~
493 ~~0.28 and 0.52 for all months except April, May and November when it is lower, whereas r is~~
494 ~~always < 0.25 when comparing with MISR (Fig. 5b).~~ ~~As for AOD, we computed the~~

495 ~~Spearman's rank correlation coefficient to reduce the possible bias due to few outliers and the~~
496 ~~smaller sample size in MISR data (N varies between 2300–5500 depending on the month and is~~
497 ~~approximately 5 times smaller than the sample size for MODIS).~~ The AE RMSD relative to
498 MODIS or MISR does not exhibit a clear seasonal pattern and the ratio of spatial standard
499 deviations in the AE fields is always lower than 1, indicating more spatial variability in the
500 satellite retrievals than in WRF-Chem. The degree to which these results are symptomatic of
501 the difficulties in retrieving AE from the remote sensing observations is unclear. When the AE
502 values are treated as binary samples ($AE < 1$ indicating coarse mode aerosols dominate, while
503 $AE > 1$ indicating a dominance of the fine mode) and presented as a contingency table, WRF-
504 Chem and MODIS simultaneously identify coarse mode dominance (i.e. $AE < -1$) in 18% of
505 grid cells (Table 5). ~~After cloud screening,~~ WRF-Chem simulates 31% of grid cells as
506 exhibiting annual mean $AE > 1$, while MODIS indicates a larger fraction of grid cells with AE
507 > 1 (80%, Table 5). Both WRF-Chem and MODIS indicate the highest prevalence of fine mode
508 particles during the warm months with highest agreement for co-identification (above 50%)
509 during June-September. Co-identification of coarse mode particles is highest in the winter and
510 spring months (above 20% during February-May and December, Table 5). However, when a χ^2
511 test is applied to the frequency of fine and coarse particles identified by WRF-Chem and
512 MODIS, for all months except January and April, the p-value is < 0.01 , thus we reject the null
513 hypothesis of equal distribution of fine and coarse mode particles identified by MODIS and
514 WRF-Chem. The two data sets agree on 29% of the cases when trying to identify fine mode
515 particles and approximately 53% of the cells are misclassified with MODIS usually identifying
516 a high prevalence of fine aerosols than WRF-Chem. AE from WRF-Chem is also negatively
517 biased relative to AERONET observations, with MFB = -0.59 indicating ~~WRF-Chem is~~
518 ~~simulating~~ a greater prevalence of coarse mode aerosols in the simulations (Table 3, Fig. 2 ~~and~~
519 ~~Fig. 4b~~).
520 EQQ plots for all sites show good accord between WRF-Chem and AERONET observations,
521 as indicated by the relatively consistent fractional error across the entire range of simulated and
522 observed AE (Fig. ~~6b~~9b). Simulations from previous studies have also shown a systematic
523 negative bias of simulated AE versus MODIS observations. AE is very difficult to derive from
524 the MODIS measurements and the uncertainty in AE scales with AOD (AE is very uncertain at
525 AOD < 0.2). Further, AE is derived from wavelength dependent AOD, thus the uncertainties
526 on the measurements are certainly correlated. As indicated in Figure 5, for some AERONET
527 sites there is evidence that positive bias in AOD is associated with high negative bias in AE,

528 but this does not uniformly occur over eastern North America (e.g. for the site at 77.8W 55.3N
529 WRF-Chem exhibits positive bias in AOD across the entire pdf while the simulated AE is
530 negative biased, but the site at 84.28W 35.95N exhibits relative good accord for AOD but is
531 negative biased in AE almost to the same amount as the northern station). -Highest biases have
532 been noted in regions dominated by dust aerosols or when the model overestimates the dust
533 loading, since aerosol population mean diameter is inversely proportional to AE (Colarco et al.,
534 2014; Balzarini et al., 2014). Sources of the biases in our study, include the simplified treatment
535 of the size distribution, weaknesses in the emission inventory or uncertainties in meteorological
536 variables affecting particle growth (e.g. temperature and relative humidity). Future work will
537 focus on examining these sensitivities.

538 **3.3 AOD Extremes**

539 Averaged across the entire simulation period, WRF-Chem correctly identifies 70% of locations
540 with extreme and non-extreme AOD in the MODIS observations (i.e. the Accuracy = 70%,
541 Table 6). The overall *TS* and *HR* also indicate the geographic location of extreme AOD is
542 similar between the model and satellite retrievals. The annual mean *HR*, which is defined as the
543 proportion of grid cells with extreme AOD co-identified by WRF-Chem and MODIS relative
544 to MODIS extremes, is 41%. The annual mean *TS*, which also takes into account false alarms,
545 is 27% (Table 6).

546 For each month, the *HR* is significantly higher than the probability of co-identification of

547 extremes by random chance (i.e. $p_0 = 0.25^2 = 0.0625$), since the test statistic $\frac{HR - p_0^2}{\sqrt{\frac{p_0 \times (1 - p_0)}{N}}}$ is

548 always larger than the critical value at 1% (i.e. 2.575). *HR* and *TS* vary seasonally, with highest
549 skill during summer months (*HR* up to 70% and *TS* up to 54%), and lowest skill during winter
550 and early spring (minimum *HR*=29% and minimum *TS*=17%) (Table 6 and Fig. 710). The
551 relatively low skill in identifying the spatial occurrence of high AOD during winter and spring
552 may reflect the relatively low AOD and low spatial variability during this season, which means
553 'extreme' AOD may differ only marginally from the 'non-extreme' areas (see SM-Fig. 4S6 for
554 monthly comparisons of extreme area identification).

555 The spatial distribution of extreme AOD also displays some seasonality with areas of AOD >
556 p_{75} concentrated over coastal regions and the southern states during summer months and

557 smaller areas during winter and early spring (Fig. 710). Despite the relatively low simultaneous
558 identification of extremes during cold seasons, the location of extremes moves from the coast
559 to the Great Lakes region and Midwest states in both the model and MODIS (see SM-Fig. 3S6).
560 During winter and spring months WRF-Chem simulates more areas with extreme AOD over
561 coastal regions, whereas MODIS shows more spatial variability and predicts higher AOD in
562 the Great Lakes area and in the states west of Illinois. Conversely, WRF-Chem underestimates
563 areas of extreme AOD relative to MODIS in the northern regions of the domain, possibly due
564 to the underestimation of sulfate-aerosol. These two observations may be explained by noting
565 that the mass fraction of aerosol nitrate in the accumulation and coarse mode predicted by WRF-
566 Chem during most of fall and winter months dominates the sulfate fraction over virtually all of
567 the domain (see SM-Fig. 5S3), whereas point observations indicate aerosol nitrate mass fraction
568 is dominant only over the Central Great Plains (Hand et al., 2012). This may be related to an
569 overestimation of aerosol-nitrate in winter and fall (Fig. 4) as a result of the impact of air
570 temperature and relative humidity on aerosol ammonium nitrate (NH_4NO_3) stability
571 (Aksoyoglu et al., 2011), as well as an underestimation of aerosol sulfate, mostly during winter
572 (Fig. 4), likely due to underestimation of the rate of SO_2 gaseous and aqueous (missing)
573 oxidation, or underestimation of the nighttime boundary layer height which impacts sulfate
574 formation near the surface (Tuccella et al., 2012). Localized negative biases in the model over
575 the coast may be associated with the higher uncertainties in MODIS retrievals at coastlines
576 (Anderson et al., 2013).

577 Extreme AOD exhibits relatively large spatial scales of coherence in both the WRF-Chem
578 simulations and MODIS L2 observations (Fig. 811). Consistent with prior analyses of L3
579 MODIS data (Sullivan et al., 2015), the largest scales of coherence are found in fall. In all
580 seasons except ~~for~~ winter the probability of co-occurrence of extremes at the domain center and
581 any other grid cell in the simulation domain is > 0.5 up to a distance of 300 km. The simulated
582 mean seasonal scales of extreme coherence are comparable to L2 MODIS AOD (Fig. 811),
583 despite the larger variability in the MODIS data due to the limited retrievals with simultaneous
584 extreme AOD at the reference location and each other grid cell. Thus, consistent with prior
585 research this analysis indicates the occurrence of extreme AOD occurs on large spatial scales
586 and therefore may significantly impact regional climate.

587 4. Discussion and concluding remarks

588 Aerosol direct and indirect radiative forcing on the climate system are highly uncertain. A
589 systematic assessment of the ability of global and regional models to reproduce aerosol optical
590 properties in the contemporary climate is essential to increasing confidence in future
591 projections. We contribute to this growing literature by presenting high resolution (12 km)
592 simulations from WRF-Chem conducted over eastern North America during a year
593 representative of average meteorological and aerosol conditions. We evaluate the simulations
594 relative to, and compare the results with daily MODIS and MISR observations, highas well as
595 with high frequency AERONET measurements of AOD and AE and near-surface PM_{2.5} mass
596 and composition measurements. -Results from this study show:

597 • After grid cells with any cloud presence are removed and considering only overpass
598 hours, the domain averaged simulated mean AOD is 0.22. Simulated AOD is positively
599 biased relative to observations, with MFB=0.14 when comparing with MODIS-Aqua
600 and 0.39-50 relative to AERONET (Fig. 2-1 and 42). A clear north-south gradient in
601 AOD bias vs. MODIS is also observed. This positive bias is consistent across the entire
602 probability distribution at most AERONET stations (Fig. 69), and is also evident in
603 comparison of modeled near-surface PM_{2.5} mass relative to daily mean observations
604 distributed at 1230 stations across the domain (Fig. 3).

605 —Model skill in reproducing the spatial fields of monthly mean AOD as measured by the
606 spatial correlation and ratio of the spatial variability with MODIS is maximized during
607 the summer months ($r \sim 0.5-0.7$, and ratio of $\sigma \sim 0.8$ to 1.2). During this season observed
608 AOD is higher and more observations are available (Fig. 57). Lowest model-
609 observations agreement is found in September and October and is at least partially
610 attributable to a dry bias in precipitation from WRF-Chem (~~SM~~Fig. 3S4).

611 •
612 • In part because of the difficulties in retrieving robust estimates of AE, few previous
613 studies have evaluated model simulated AE values. We show that AE as simulated by
614 WRF-Chem over eastern North America is negatively biased relative to MODIS
615 (MFB=-0.10) and AERONET (MFB=-0.6459). This bias indicates WRF-Chem
616 simulates a larger fraction of coarse mode particles than is evident in the remote sensing
617 observations (see Table 3 and 5). While some of the bias relative to MODIS may reflect
618 high observational uncertainty, the- large bias relative to AERONET is consistent with

619 prior research (Table 1), and is symptomatic of substantial systematic error in the
620 aerosol size distribution.

- 621 • ~~the bias relative to AERONET is consistent with prior research (Table 1) and is~~
622 ~~symptomatic of relatively poor model performance for this metric.~~ Causes of the model
623 error may include insufficiently detailed treatment of size distribution or inaccurate
624 representation of aerosol composition and mixing state which affect the simulated size
625 distribution and thus AE (Li et al., 2015;Curci et al., 2014)). Further, weaknesses in the
626 emission inventory (e.g. size resolution of primary emissions), as suggested by the
627 systematic bias in simulated PM_{2.5} concentrations relative to ground-based observations,
628 and/or biases in the representation of meteorological conditions critical to determining
629 aerosol nitrate concentrations may also affect model performance. Currently it is not
630 possible to fully attribute the relative importance of these error sources.
- 631 • The majority of prior model evaluation exercises have tended to focus on mean AOD
632 values~~the central tendency of the AOD probability distribution~~. However, the climate
633 and health impacts of aerosols are maximized-greater under high aerosol loadings. We
634 demonstrate that WRF-Chem exhibits some skill in capturing the spatial patterns of
635 extreme aerosol loading, especially during summer months. During this season, the Hit
636 Rate for AOD > p75 reaches 70%. Largest biases are found during winter months and
637 near the coastlines where AOD from MODIS also exhibits largest retrieval uncertainty.

638 Despite the encouraging performance of WRF-Chem both in terms of simulation efficiency and
639 in reproducing AOD (mean and extreme values) and the partial skill in reproducing AE over
640 eastern North America, further investigations are needed to properly quantify the value added
641 by running high-resolution simulations by direct comparison with analogous runs at coarser
642 resolution. Future simulations will also involve assessment of accuracy of different aerosol
643 schemes (i.e. sectional vs. modal approaches) to represent the size distribution. The inclusion
644 of a direct description of new particle formation processes within WRF-Chem may also
645 improve estimates of ultrafine particle concentrations and thus of simulated aerosol optical
646 properties.

647 **5. Acknowledgements**

648 This research was supported in part by Lilly Endowment, Inc., through its support for the
649 Indiana University Pervasive Technology Institute, and in part by the Indiana METACyt
650 Initiative. The Indiana METACyt Initiative at IU is also supported in part by Lilly Endowment,

651 Inc. Additional support was provided by the L'Oréal-UNESCO UK and Ireland Fellowship For
652 Women In Science (to PC), the Natural Environmental Research Council (NERC) through the
653 LICS project (ref. NE/K010794/1), the US NSF (grants # 1102309 and 1517365 to SCP) and
654 a NASA Earth and Space Science Fellowship Program - Grant "14-EARTH14F-0207" (to
655 RCS). The data used in this study were acquired as part of the NASA's Earth-Sun System
656 Division, and archived and distributed by the MODIS Level 1 and Atmosphere Archive and
657 Distribution System (LAADS), and the Giovanni online data system, developed and maintained
658 by the NASA Goddard Earth Sciences (GES) Data and Information Services Center (DISC).
659 We thank the PI investigators and their staff for establishing and maintaining the 22 AERONET
660 sites used in this investigation. PM_{2.5} surface concentrations from the United States
661 Environmental Protection Agency were obtained from:
662 http://www.epa.gov/airquality/airdata/ad_data_daily.html. Meteorological lateral boundary
663 conditions from the North American Mesoscale model were obtained from the NOAA
664 Operational Model Archive and Distribution System:
665 ftp://nomads.ncdc.noaa.gov/NAM/analysis_only/.

666

667 6. References

- 668 Ackermann, I. J., Hass, H., Memmesheimer, M., Ebel, A., Binkowski, F. S., and Shankar, U.:
669 Modal aerosol dynamics model for Europe: development and first applications, *Atmos.*
670 *Environ.*, 32, 2981-2999, [http://dx.doi.org/10.1016/S1352-2310\(98\)00006-5](http://dx.doi.org/10.1016/S1352-2310(98)00006-5), 1998.
- 671 Aksoyoglu, S., Keller, J., Barmpadimos, I., Oderbolz, D., Lanz, V. A., Prévôt, A. S. H., and
672 Baltensperger, U.: Aerosol modelling in Europe with a focus on Switzerland during summer
673 and winter episodes, *Atmos. Chem. Phys.*, 11, 7355-7373, 10.5194/acp-11-7355-2011, 2011.
- 674 Alston, E. J., Sokolik, I. N., and Kalashnikova, O. V.: Characterization of atmospheric aerosol
675 in the US Southeast from ground- and space-based measurements over the past decade,
676 *Atmospheric Measurement Techniques*, 5, 1667-1682, 10.5194/amt-5-1667-2012, 2012.
- 677 Anderson, J. C., Wang, J., Zeng, J., Leptoukh, G., Petrenko, M., Ichoku, C., and Hu, C.: Long-
678 term statistical assessment of Aqua-MODIS aerosol optical depth over coastal regions: bias
679 characteristics and uncertainty sources, *Tellus Series B-Chemical and Physical Meteorology*,
680 65, 10.3402/tellusb.v65i0.20805, 2013.
- 681 Anderson, J. R., Hardy, E. E., Roach, J. T., and Witmer, R. E.: A land use and land cover
682 classification system for use with remote sensor data, Report 964, 1976.
- 683 Anderson, T. L., Charlson, R. J., Winker, D. M., Ogren, J. A., and Holmén, K.: Mesoscale
684 Variations of Tropospheric Aerosols*, *Journal of the Atmospheric Sciences*, 60, 119-136,
685 10.1175/1520-0469(2003)060<0119:MVOTA>2.0.CO;2, 2003.
- 686 Balzarini, A., Pirovano, G., Honzak, L., Žabkar, R., Curci, G., Forkel, R., Hirtl, M., San José,
687 R., Tuccella, P., and Grell, G. A.: WRF-Chem model sensitivity to chemical mechanisms choice

688 in reconstructing aerosol optical properties, *Atmos. Environ.*,
689 <http://dx.doi.org/10.1016/j.atmosenv.2014.12.033>, 2014.

690 Boucher, O., D. Randall, and P. Artaxo, C. B., G. Feingold, P. Forster, V.-M. Kerminen, Y.
691 Kondo, H. Liao, U. Lohmann, P. Rasch, S.K. Satheesh, S. Sherwood, B. Stevens and X.Y.
692 Zhang: Clouds and Aerosols, in: *Climate Change 2013: The Physical Science Basis.*
693 Contribution of Working Group I to the Fifth Assessment Report of the Intergovernmental
694 Panel on Climate Change, edited by: Stocker, T. F., D. Qin, G.-K. Plattner, M. Tignor, S.K.
695 Allen, J. Boschung, A. Nauels, Y. Xia, V. Bex and P.M. Midgley, Cambridge University Press,
696 Cambridge, United Kingdom and New York, NY, USA, 33–115, 2013.

697 Boylan, J. W., and Russell, A. G.: PM and light extinction model performance metrics, goals,
698 and criteria for three-dimensional air quality models, *Atmos. Environ.*, 40, 4946-4959,
699 <http://dx.doi.org/10.1016/j.atmosenv.2005.09.087>, 2006.

700 Castro, C. L., Pielke, R. A., and Leoncini, G.: Dynamical downscaling: Assessment of value
701 retained and added using the Regional Atmospheric Modeling System (RAMS), *Journal of*
702 *Geophysical Research: Atmospheres*, 110, D05108, 10.1029/2004JD004721, 2005.

703 Chu, S. H.: PM_{2.5} episodes as observed in the speciation trends network, *Atmos. Environ.*, 38,
704 5237-5246, 10.1016/j.atmosenv.2004.01.055, 2004.

705 Colarco, P., da Silva, A., Chin, M., and Diehl, T.: Online simulations of global aerosol
706 distributions in the NASA GEOS-4 model and comparisons to satellite and ground-based
707 aerosol optical depth, *J. Geophys. Res.-Atmos.*, 115, 10.1029/2009jd012820, 2010.

708 Colarco, P., Kahn, R. A., Remer, L. A., and Levy, R. C.: Impact of satellite viewing-swath
709 width on global and regional aerosol optical thickness statistics and trends, *Atmospheric*
710 *Measurement Techniques*, 7, 2313-2335, 10.5194/amt-7-2313-2014, 2014.

711

712 Curci, G., Hogrefe, C., Bianconi, R., Im, U., Balzarini, A., Baró, R., Brunner, D., Forkel, R.,
713 Giordano, L., Hirtl, M., Honzak, L., Jiménez-Guerrero, P., Knote, C., Langer, M., Makar, P.
714 A., Pirovano, G., Pérez, J. L., San José, R., Syrakov, D., Tuccella, P., Werhahn, J., Wolke, R.,
715 Žabkar, R., Zhang, J., and Galmarini, S.: Uncertainties of simulated aerosol optical properties
716 induced by assumptions on aerosol physical and chemical properties: An AQMEII-2
717 perspective, *Atmos. Environ.*, <http://dx.doi.org/10.1016/j.atmosenv.2014.09.009>, 2014.

718 de Meij, A., Pozzer, A., Pringle, K. J., Tost, H., and Lelieveld, J.: EMAC model evaluation and
719 analysis of atmospheric aerosol properties and distribution with a focus on the Mediterranean
720 region, *Atmospheric Research*, 114–115, 38-69,
721 <http://dx.doi.org/10.1016/j.atmosres.2012.05.014>, 2012.

722 Drury, E., Jacob, D. J., Spurr, R. J. D., Wang, J., Shinozuka, Y., Anderson, B. E., Clarke, A.
723 D., Dibb, J., McNaughton, C., and Weber, R.: Synthesis of satellite (MODIS), aircraft
724 (ICARTT), and surface (IMPROVE, EPA-AQS, AERONET) aerosol observations over eastern
725 North America to improve MODIS aerosol retrievals and constrain surface aerosol
726 concentrations and sources, *J. Geophys. Res.-Atmos.*, 115, 10.1029/2009jd012629, 2010.

727 Emmons, L. K., Walters, S., Hess, P. G., Lamarque, J. F., Pfister, G. G., Fillmore, D., Granier,
728 C., Guenther, A., Kinnison, D., Laepple, T., Orlando, J., Tie, X., Tyndall, G., Wiedinmyer, C.,
729 Baughcum, S. L., and Kloster, S.: Description and evaluation of the Model for Ozone and
730 Related chemical Tracers, version 4 (MOZART-4), *Geoscientific Model Development*, 3, 43-
731 67, 2010.

732 Fast, J. D., Gustafson, W. I., Easter, R. C., Zaveri, R. A., Barnard, J. C., Chapman, E. G., Grell,
733 G. A., and Peckham, S. E.: Evolution of ozone, particulates, and aerosol direct radiative forcing
734 in the vicinity of Houston using a fully coupled meteorology-chemistry-aerosol model, *Journal*
735 *of Geophysical Research: Atmospheres*, 111, D21305, 10.1029/2005JD006721, 2006.

736 Ford, B., and Heald, C. L.: Aerosol loading in the Southeastern United States: reconciling
737 surface and satellite observations, *Atmospheric Chemistry and Physics*, 13, 9269-9283,
738 10.5194/acp-13-9269-2013, 2013.

739 Giannouli, M., Kalognomou, E.-A., Mellios, G., Moussiopoulos, N., Samaras, Z., and Fiala, J.:
740 Impact of European emission control strategies on urban and local air quality, *Atmos. Environ.*,
741 45, 4753-4762, 10.1016/j.atmosenv.2010.03.016, 2011.

742 Gkikas, A., Houssos, E. E., Hatzianastassiou, N., Papadimas, C. D., and Bartzokas, A.: Synoptic
743 conditions favouring the occurrence of aerosol episodes over the broader Mediterranean basin,
744 *Quarterly Journal of the Royal Meteorological Society*, 138, 932-949, 10.1002/qj.978, 2012.

745 Grell, G. A., Peckham, S. E., Schmitz, R., McKeen, S. A., Frost, G., Skamarock, W. C., and
746 Eder, B.: Fully coupled "online" chemistry within the WRF model, *Atmos. Environ.*, 39, 6957-
747 6975, 10.1016/j.atmosenv.2005.04.027, 2005.

748 Guenther, A., Zimmerman, P., and Wildermuth, M.: Natural volatile organic compound
749 emission rate estimates for U.S. woodland landscapes, *Atmos. Environ.*, 28, 1197-1210,
750 10.1016/1352-2310(94)90297-6, 1994.

751 Guenther, A. B., Zimmerman, P. R., Harley, P. C., Monson, R. K., and Fall, R.: Isoprene and
752 monoterpene emission rate variability: model evaluations and sensitivity analyses, *J. Geophys.*
753 *Res.-Atmos.*, 98, 12609-12617, 10.1029/93jd00527, 1993.

754 [Kovacs, T. \(2006\). "Comparing MODIS and AERONET aerosol optical depth at varying](#)
755 [separation distances to assess ground-based validation strategies for spaceborne lidar." *J.*](#)
756 [*Geophys. Res-Atmos.* 111\(D24\).](#)

757

758 Hand, J. L., Schichtel, B. A., Pitchford, M., Malm, W. C., and Frank, N. H.: Seasonal
759 composition of remote and urban fine particulate matter in the United States, *Journal of*
760 *Geophysical Research: Atmospheres*, 117, D05209, 10.1029/2011JD017122, 2012.

761 [Hyer, E. J., Reid, J. S., and Zhang, J.: An over-land aerosol optical depth data set for data](#)
762 [assimilation by filtering, correction, and aggregation of MODIS Collection 5 optical depth](#)
763 [retrievals, *Atmospheric Measurement Techniques*, 4, 379-408, 10.5194/amt-4-379-2011, 2011.](#)

764

765 Holben, B. N., Eck, T. F., Slutsker, I., Tanre, D., Buis, J. P., Setzer, A., Vermote, E., Reagan,
766 J. A., Kaufman, Y. J., Nakajima, T., Lavenu, F., Jankowiak, I., and Smirnov, A.: AERONET -
767 A federated instrument network and data archive for aerosol characterization, *Remote Sensing*
768 *of Environment*, 66, 1-16, 10.1016/s0034-4257(98)00031-5, 1998.

769 Holben, B. N., Tanre, D., Smirnov, A., Eck, T. F., Slutsker, I., Abuhassan, N., Newcomb, W.
770 W., Schafer, J. S., Chatenet, B., Lavenu, F., Kaufman, Y. J., Castle, J. V., Setzer, A., Markham,
771 B., Clark, D., Frouin, R., Halthore, R., Karneli, A., O'Neill, N. T., Pietras, C., Pinker, R. T.,
772 Voss, K., and Zibordi, G.: An emerging ground-based aerosol climatology: Aerosol optical
773 depth from AERONET, *J. Geophys. Res.-Atmos.*, 106, 12067-12097, 10.1029/2001jd900014,
774 2001.

775 Kahn, R. A., Gaitley, B. J., Martonchik, J. V., Diner, D. J., Crean, K. A., and Holben, B.:
776 Multiangle Imaging Spectroradiometer (MISR) global aerosol optical depth validation based
777 on 2 years of coincident Aerosol Robotic Network (AERONET) observations, *J. Geophys.*
778 *Res.-Atmos.*, 110, 10.1029/2004jd004706, 2005.

779 Kahn, R. A., Gaitley, B. J., Garay, M. J., Diner, D. J., Eck, T. F., Smirnov, A., and Holben, B.
780 N.: Multiangle Imaging SpectroRadiometer global aerosol product assessment by comparison
781 with the Aerosol Robotic Network, *J. Geophys. Res.-Atmos.*, 115, 10.1029/2010jd014601,
782 2010.

783 Kinne, S., O'Donnel, D., Stier, P., Kloster, S., Zhang, K., Schmidt, H., Rast, S., Giorgetta, M.,
784 Eck, T. F., and Stevens, B.: MAC-v1: A new global aerosol climatology for climate studies,
785 *Journal of Advances in Modeling Earth Systems*, 5, 704-740, 10.1002/jame.20035, 2013.

786 Kulmala, M., Asmi, A., Lappalainen, H. K., Baltensperger, U., Brenguier, J. L., Facchini, M.
787 C., Hansson, H. C., Hov, O., O'Dowd, C. D., Poeschl, U., Wiedensohler, A., Boers, R., Boucher,
788 O., de Leeuw, G., van der Gon, H. A. C. D., Feichter, J., Krejci, R., Laj, P., Lihavainen, H.,
789 Lohmann, U., McFiggans, G., Mentel, T., Pilinis, C., Riipinen, I., Schulz, M., Stohl, A.,
790 Swietlicki, E., Vignati, E., Alves, C., Amann, M., Ammann, M., Arabas, S., Artaxo, P., Baars,
791 H., Beddows, D. C. S., Bergstrom, R., Beukes, J. P., Bilde, M., Burkhardt, J. F., Canonaco, F.,
792 Clegg, S. L., Coe, H., Crumeyrolle, S., D'Anna, B., Decesari, S., Gilardoni, S., Fischer, M.,
793 Fjaeraa, A. M., Fountoukis, C., George, C., Gomes, L., Halloran, P., Hamburger, T., Harrison,
794 R. M., Herrmann, H., Hoffmann, T., Hoose, C., Hu, M., Hyvarinen, A., Horrak, U., Iinuma, Y.,
795 Iversen, T., Josipovic, M., Kanakidou, M., Kiendler-Scharr, A., Kirkevag, A., Kiss, G.,
796 Klimont, Z., Kolmonen, P., Komppula, M., Kristjansson, J. E., Laakso, L., Laaksonen, A.,
797 Labonnote, L., Lanz, V. A., Lehtinen, K. E. J., Rizzo, L. V., Makkonen, R., Manninen, H. E.,
798 McMeeking, G., Merikanto, J., Minikin, A., Mirme, S., Morgan, W. T., Nemitz, E., O'Donnell,
799 D., Panwar, T. S., Pawlowska, H., Petzold, A., Pienaar, J. J., Pio, C., Plass-Duelmer, C., Prevo,
800 A. S. H., Pryor, S., Reddington, C. L., Roberts, G., Rosenfeld, D., Schwarz, J., Seland, O.,
801 Sellegri, K., Shen, X. J., Shiraiwa, M., Siebert, H., Sierau, B., Simpson, D., Sun, J. Y., Topping,
802 D., Tunved, P., Vaattovaara, P., Vakkari, V., Veefkind, J. P., Visschedijk, A., Vuollekoski, H.,
803 Vuolo, R., Wehner, B., Wildt, J., Woodward, S., Worsnop, D. R., van Zadelhoff, G. J., Zardini,
804 A. A., Zhang, K., van Zyl, P. G., Kerminen, V. M., Carslaw, K. S., and Pandis, S. N.: General
805 overview: European Integrated project on Aerosol Cloud Climate and Air Quality interactions
806 (EUCAARI) - integrating aerosol research from nano to global scales, *Atmospheric Chemistry*
807 *and Physics*, 11, 13061-13143, 10.5194/acp-11-13061-2011, 2011.

808 Kumar, R., Barth, M. C., Pfister, G. G., Naja, M., and Brasseur, G. P.: WRF-Chem simulations
809 of a typical pre-monsoon dust storm in northern India: influences on aerosol optical properties
810 and radiation budget, *Atmospheric Chemistry and Physics*, 14, 2431-2446, 10.5194/acp-14-
811 2431-2014, 2014.

812 Kurokawa, J., Ohara, T., Morikawa, T., Hanayama, S., Janssens-Maenhout, G., Fukui, T.,
813 Kawashima, K., and Akimoto, H.: Emissions of air pollutants and greenhouse gases over Asian
814 regions during 2000-2008: Regional Emission inventory in ASia (REAS) version 2,
815 *Atmospheric Chemistry and Physics*, 13, 11019-11058, 10.5194/acp-13-11019-2013, 2013.

816 Lee, Y. H., Adams, P. J., and Shindell, D. T.: Evaluation of the global aerosol microphysical
817 ModelE2-TOMAS model against satellite and ground-based observations, *Geosci. Model Dev.*,
818 8, 631-667, 10.5194/gmd-8-631-2015, 2015.

819 Levy, R. C., Remer, L. A., and Dubovik, O.: Global aerosol optical properties and application
820 to Moderate Resolution Imaging Spectroradiometer aerosol retrieval over land, *J. Geophys.*
821 *Res.-Atmos.*, 112, 15, 10.1029/2006jd007815, 2007.

822 Levy, R. C., Remer, L. A., Kleidman, R. G., Mattoo, S., Ichoku, C., Kahn, R., and Eck, T. F.:
823 Global evaluation of the Collection 5 MODIS dark-target aerosol products over land,
824 *Atmospheric Chemistry and Physics*, 10, 10399-10420, 10.5194/acp-10-10399-2010, 2010.

825 Li, S., Kahn, R., Chin, M., Garay, M. J., and Liu, Y.: Improving satellite-retrieved aerosol
826 microphysical properties using GOCART data, *Atmos. Meas. Tech.*, 8, 1157-1171,
827 10.5194/amt-8-1157-2015, 2015.

828 Matsuura, K., and Willmott, C. J.: Terrestrial precipitation: 1900–2008 gridded monthly time
829 series, 2009.

830 Michou, M., Nabat, P., and Saint-Martin, D.: Development and basic evaluation of a prognostic
831 aerosol scheme (v1) in the CNRM Climate Model CNRM-CM6, *Geosci. Model Dev.*, 8, 501-
832 531, 10.5194/gmd-8-501-2015, 2015.

833 Myhre, G., Samset, B. H., Schulz, M., Balkanski, Y., Bauer, S., Berntsen, T. K., Bian, H.,
834 Bellouin, N., Chin, M., Diehl, T., Easter, R. C., Feichter, J., Ghan, S. J., Hauglustaine, D.,
835 Iversen, T., Kinne, S., Kirkevåg, A., Lamarque, J. F., Lin, G., Liu, X., Lund, M. T., Luo, G.,
836 Ma, X., van Noije, T., Penner, J. E., Rasch, P. J., Ruiz, A., Seland, O., Skeie, R. B., Stier, P.,
837 Takemura, T., Tsigaridis, K., Wang, P., Wang, Z., Xu, L., Yu, H., Yu, F., Yoon, J. H., Zhang,
838 K., Zhang, H., and Zhou, C.: Radiative forcing of the direct aerosol effect from AeroCom Phase
839 II simulations, *Atmospheric Chemistry and Physics*, 13, 1853-1877, 10.5194/acp-13-1853-
840 2013, 2013.

841 Nabat, P., Somot, S., Mallet, M., Michou, M., Sevault, F., Driouech, F., Meloni, D., di Sarra,
842 A., Di Biagio, C., Formenti, P., Sicard, M., Léon, J. F., and Bouin, M. N.: Dust aerosol radiative
843 effects during summer 2012 simulated with a coupled regional aerosol–atmosphere–ocean
844 model over the Mediterranean, *Atmos. Chem. Phys.*, 15, 3303-3326, 10.5194/acp-15-3303-
845 2015, 2015.

846 Nair, V. S., Solmon, F., Giorgi, F., Mariotti, L., Babu, S. S., and Moorthy, K. K.: Simulation of
847 South Asian aerosols for regional climate studies, *Journal of Geophysical Research:*
848 *Atmospheres*, 117, n/a-n/a, 10.1029/2011JD016711, 2012.

849 Pereira, S. N., Wagner, F., and Silva, A. M.: Seven years of measurements of aerosol scattering
850 properties, near the surface, in the southwestern Iberia Peninsula, *Atmospheric Chemistry and*
851 *Physics*, 11, 17-29, 10.5194/acp-11-17-2011, 2011.

852 Pfister, G. G., Parrish, D. D., Worden, H., Emmons, L. K., Edwards, D. P., Wiedinmyer, C.,
853 Diskin, G. S., Huey, G., Oltmans, S. J., Thouret, V., Weinheimer, A., and Wisthaler, A.:
854 Characterizing summertime chemical boundary conditions for airmasses entering the US West
855 Coast, *Atmos. Chem. Phys.*, 11, 1769-1790, 10.5194/acp-11-1769-2011, 2011.

856 Rea, G., Turquety, S., Menut, L., Briant, R., Mailler, S., and Siour, G.: Source contributions to
857 2012 summertime aerosols in the Euro-Mediterranean region, *Atmos. Chem. Phys. Discuss.*,
858 15, 8191-8242, 10.5194/acpd-15-8191-2015, 2015.

859 Remer, L. A., Kaufman, Y. J., Tanre, D., Mattoo, S., Chu, D. A., Martins, J. V., Li, R. R.,
860 Ichoku, C., Levy, R. C., Kleidman, R. G., Eck, T. F., Vermote, E., and Holben, B. N.: The
861 MODIS aerosol algorithm, products, and validation, *Journal of the Atmospheric Sciences*, 62,
862 947-973, 10.1175/jas3385.1, 2005.

863 Schell, B., Ackermann, I. J., Hass, H., Binkowski, F. S., and Ebel, A.: Modeling the formation
864 of secondary organic aerosol within a comprehensive air quality model system, *J. Geophys.*
865 *Res.-Atmos.*, 106, 28275-28293, 10.1029/2001jd000384, 2001.

866 Shepard, D.: A two-dimensional interpolation function for irregularly-spaced data, *Proceedings*
867 *of the 1968 23rd ACM national conference*, 1968.

868 Sič, B., El Amraoui, L., Marécal, V., Josse, B., Arteta, J., Guth, J., Joly, M., and Hamer, P. D.:
869 Modelling of primary aerosols in the chemical transport model MOCAGE: development and
870 evaluation of aerosol physical parameterizations, *Geosci. Model Dev.*, 8, 381-408,
871 10.5194/gmd-8-381-2015, 2015.

872 Simpson, D., Guenther, A., Hewitt, C. N., and Steinbrecher, R.: Biogenic emissions in Europe.
873 1. estimates and uncertainties, *J. Geophys. Res.-Atmos.*, 100, 22875-22890,
874 10.1029/95jd02368, 1995.

875 Spracklen, D. V., Carslaw, K. S., Merikanto, J., Mann, G. W., Reddington, C. L., Pickering, S.,
876 Ogren, J. A., Andrews, E., Baltensperger, U., Weingartner, E., Boy, M., Kulmala, M., Laakso,
877 L., Lihavainen, H., Kivekäs, N., Komppula, M., Mihalopoulos, N., Kouvarakis, G., Jennings,
878 S. G., O'Dowd, C., Birmili, W., Wiedensohler, A., Weller, R., Gras, J., Laj, P., Sellegri, K.,
879 Bonn, B., Krejci, R., Laaksonen, A., Hamed, A., Minikin, A., Harrison, R. M., Talbot, R., and
880 Sun, J.: Explaining global surface aerosol number concentrations in terms of primary emissions
881 and particle formation, *Atmos. Chem. Phys.*, 10, 4775-4793, 10.5194/acp-10-4775-2010, 2010.

882 Stocker, T. F., Qin, D., and Plattner, G.-K., Alexander, L.V., Allen, S.K., Bindoff, N.L., Bréon,
883 F.-M., Church, J.A., Cubasch, U., Emori, S., Forster, P., Friedlingstein, P., Gillett, N., Gregory,
884 J.M., Hartmann, D.L., Jansen, E., Kirtman, B., Knutti, R., Krishna Kumar, K. and Lemke, P.
885 and Marotzke, J., Masson-Delmotte, V., Meehl, G.A., Mokhov, I.I., Piao, S., Ramaswamy,
886 V., Randall, D., Rhein, M., Rojas, M., Sabine, C., Shindell, D., Talley, L.D., Vaughan, D.G.,
887 Xie, S.-P.: Summary for Policymakers, in: *Climate Change 2013: The Physical Science Basis.*
888 *Contribution of Working Group I to the Fifth Assessment Report of the Intergovernmental*
889 *Panel on Climate Change*, Cambridge University Press, Cambridge, United Kingdom and New
890 York, NY, USA, 33–115, 2013.

891 [Santese, M., F. De Tomasi and M. R. Perrone \(2007\). "AERONET versus MODIS aerosol](#)
892 [parameters at different spatial resolutions over southeast Italy." *J. Geophys. Res.-Atmos.*](#)
893 [112\(D10\).](#)

894 [Schutgens, N. A. J., M. Nakata and T. Nakajima \(2013\). "Validation and empirical correction](#)
895 [of MODIS AOT and AE over ocean." *Atmos. Meas. Techn.* 6\(9\): 2455-2475.](#)

896 [Shinozuka, Y. and J. Redemann \(2011\). "Horizontal variability of aerosol optical depth](#)
897 [observed during the ARCTAS airborne experiment." *Atmos. Chem. Phys.* 11\(16\): 8489-8495.](#)

898 Stockwell, W. R., Middleton, P., Chang, J. S., and Tang, X.: The second generation regional
899 acid deposition model chemical mechanism for regional air quality modeling, *Journal of*
900 *Geophysical Research: Atmospheres*, 95, 16343-16367, 10.1029/JD095iD10p16343, 1990.

901 Sullivan, R. C., Levy, R. C., and Pryor, S. C.: Spatiotemporal coherence of mean and extreme
902 aerosol particle events over eastern North America as observed from satellite, *Atmos. Environ.*,
903 112, 126-135, <http://dx.doi.org/10.1016/j.atmosenv.2015.04.026>, 2015.

904 Taylor, K. E.: Summarizing multiple aspects of model performance in a single diagram, *J.*
905 *Geophys. Res.-Atmos.*, 106, 7183-7192, 10.1029/2000jd900719, 2001.

906 Tessum, C. W., Hill, J. D., and Marshall, J. D.: Twelve-month, 12 km resolution North
907 American WRF-Chem v3.4 air quality simulation: performance evaluation, *Geosci. Model*
908 *Dev. Discuss.*, 7, 8433-8476, 10.5194/gmdd-7-8433-2014, 2014.

909 Tuccella, P., Curci, G., Visconti, G., Bessagnet, B., Menut, L., and Park, R. J.: Modeling of gas
910 and aerosol with WRF/Chem over Europe: Evaluation and sensitivity study, *Journal of*
911 *Geophysical Research: Atmospheres*, 117, D03303, 10.1029/2011JD016302, 2012.

912 Tuccella, P., Curci, G., Grell, G. A., Visconti, G., Crumeyrolle, S., Schwarzenboeck, A., and
913 Mensah, A. A.: A new chemistry option in WRF/Chem v. 3.4 for the simulation of direct and
914 indirect aerosol effects using VBS: evaluation against IMPACT-EUCAARI data, *Geosci.*
915 *Model Dev. Discuss.*, 8, 791-853, 10.5194/gmdd-8-791-2015, 2015.

916 US-EPA: 2005 National Emissions Inventory (NEI), US Environmental Protection Agency
917 available at: ftp://aftp.fsl.noaa.gov/divisions/taq/emissions_data_2005/, 2009.

918 Valenzuela, A., Olmo, F. J., Lyamani, H., Granados-Munoz, M. J., Anton, M., Guerrero-
919 Rascado, J. L., Quirantes, A., Toledano, C., Perez-Ramirez, D., and Alados-Arboledas, L.:
920 Aerosol transport over the western Mediterranean basin: Evidence of the contribution of fine
921 particles to desert dust plumes over Alboran Island, *J. Geophys. Res.-Atmos.*, 119, 14028-
922 14044, 10.1002/2014jd022044, 2014.

923 Willmott, C. J., Rowe, C. M., and Philpot, W. D.: Small-Scale Climate Maps: A Sensitivity
924 Analysis of Some Common Assumptions Associated with Grid-Point Interpolation and
925 Contouring, *The American Cartographer*, 12, 5-16, 10.1559/152304085783914686, 1985.

926 Wu, S., Mickley, L. J., Kaplan, J. O., and Jacob, D. J.: Impacts of changes in land use and land
927 cover on atmospheric chemistry and air quality over the 21st century, *Atmospheric Chemistry*
928 *and Physics*, 12, 1597-1609, 10.5194/acp-12-1597-2012, 2012.

929 Xing, J., Mathur, R., Pleim, J., Hogrefe, C., Gan, C. M., Wong, D. C., Wei, C., Gilliam, R., and
930 Pouliot, G.: Observations and modeling of air quality trends over 1990-2010 across the
931 Northern Hemisphere: China, the United States and Europe, *Atmospheric Chemistry and*
932 *Physics*, 15, 2723-2747, 10.5194/acp-15-2723-2015, 2015.

933 Zhang, Y., Chen, Y., Sarwar, G., and Schere, K.: Impact of gas-phase mechanisms on Weather
934 Research Forecasting Model with Chemistry (WRF/Chem) predictions: Mechanism
935 implementation and comparative evaluation, *J. Geophys. Res.-Atmos.*, 117,
936 10.1029/2011jd015775, 2012.

937 **Tables**

938 Table 1. Synthesis of some recent prior studies comparing simulated aerosol optical properties from global or regional model simulations with
 939 remote sensing products. The first column summarizes the model used, the second the domain and the time period simulated and the third shows
 940 the model resolution and summarizes the description of the aerosol size distribution. Columns 4 to 9 summarize the evaluation statistics in terms
 941 of the overall correlation coefficient (R), bias (as described using the mean fractional error (MFE)) and root mean square error (RMSE) or mean
 942 absolute error (MAE) relative to satellite or AERONET observations as reported in the references shown in column 10.

Model	Domain, Time	Resolution, Aerosol Approach	R AOD vs. Satellite	bias AOD vs. Satellite	R AOD vs. AERONET	bias AOD vs. AERONET	R AE vs. AERONE T	RMSE, MAE AE vs. AERONET	Ref
TOMAS in GISS	Global, 2000-2003	2°x2.5°, Sectional: 15 bins from 3 nm-10 μm	0.63 (average of monthly from 2004-2006, MODIS), 0.73 average of monthly from 2004-2006, MISR)	MFE: -29% (average of monthly from 2004- 2006, MODIS), -34% (average of monthly from 2004-2006, MISR)	-0.7-0.99 (monthly, 28)	-77-72% (monthly, 28)	N/A	N/A	(Lee et al., 2015)
GOCART with GEOS DAS	CONUS, 2006-2009	1°x1.25°, not specified	N/A	N/A	0.5 (2 hr. average at MISR overpass, 32)	N/A	0.43 (2 hr. average at MISR overpass, 32)	N/A	(Li et al., 2015)

GEMS/MACC aerosol module in CNRM-GAME and CERFACS	Global, 1993-2012	1.4°, Sectional, 12 bins	N/A	Mean relative bias -41-(-52)% (monthly, MISR)	<0-0.9 (monthly, 166)	N/A	N/A	N/A	(Michou et al., 2015)
CNRM-RCSM5	Mediterr., Summer 2012	50 km, Sectional, 12 bins	0.64 (seasonal, MODIS), 0.77 (seasonal, MISR), 0.65 (seasonal SEVIRI)	N/A	0.7 (daily, 30)	RMSE~1.75 (daily, 30)	N/A	N/A	(Nabat et al., 2015)
CHIMERE chemical transport model with WRF meteorology	Europe, Mediter. -10°-40°E, 30°-55°N, Summer 2012	50 km, Sectional: 5 bins, 40 nm-40 μm	0.35-0.75 (hourly, MODIS)	RMSE: 0.04-0.1 (hourly, MODIS)	0.44-0.73 (hourly, 65)	RMSE: 0.8-0.11 (hourly, 65)	N/A	N/A	(Rea et al., 2015)
MOCAGE	Global, 2007	2°x2°, Sectional: 6 bins per species	0.322 (daily MODIS)	normalized mean bias 0.098 (daily MODIS)	N/A	N/A	N/A	N/A	(Sič et al., 2015)
WRF-Chem	0°-10°E, 50°-55°N; -10°-15°E, 46°-57°N; -15°-30°E,	nested 2 - 30 km, modal	N/A	0.38±0.12 and 0.42±0.10 domain average AOD from MODIS and model respectively	N/A	N/A	N/A	N/A	(Tuccella et al., 2015)

	36°-62°N, 14-30 May 2008								
GOCART in GEOS	Global, 2000-2006	1°x1.25°, dust (8 bins 0.1-10 µm), sea salt (5 bins 0.03-10 µm), carbonaceous/sulfate (modal)	0.747, 0.72 E.US (monthly, MODIS)	N/A	0.707 (monthly, 53)	rms: 0.133 (monthly, 53)	0.81 (monthly, 53)	rms: 0.285 (monthly, 53)	(Colarco et al., 2010)
EMAC	Global, Year 2006	1.1°x1.1°, modal	N/A	Negative (North America)	0.27-0.60 (North America)	RMSE=0.1-0.2	>0.5 (Europe)	N/A	(de Meij et al., 2012)
GEOS-Chem	N. America, 06 July - 14 Aug 2004	2°x2.5°, modal	N/A	N/A	0.87 (study period mean, 24)	N/A	N/A	N/A	(Drury et al., 2010)
WRF-Chem	Europe and N. Africa, Year 2010	23 km, Modal and sectional (4 bins: 0.04-10 µm)	N/A	N/A	0.52 (mod) 0.51 (sect)	NMB=- 0.06(mod) NMB=-0.21 (sect) (daily, 12 stations)	N/A	N/A	(Balzarini et al., 2014)
RegCM4	South Asia,	50 km,	N/A	N/A	0.47-0.71	N/A	N/A	N/A	(Nair et al., 2012)

	2005-2007	Sectional (4 bins: 0.01-20 μm)			Monthly, 6				
--	-----------	---	--	--	------------	--	--	--	--

943

944 Table 2. Physical and chemical schemes adopted in the WRF-Chem simulations presented
 945 herein.

Simulation settings	Values
Domain size	300 × 300 cells
Horizontal resolution	12 km
Vertical resolution	32 levels up to 50 hPa
Timestep for physics	72 s
Timestep for chemistry	5 s
Physics option	Adopted scheme
Microphysics	WRF Single-Moment 5-class
Longwave Radiation	Rapid Radiative Transfer Model (RRTM)
Shortwave Radiation	Goddard
Surface layer	Monin Obhukov similarity
Land Surface	Noah Land Surface Model
Planetary boundary layer	Mellor-Yamada-Janjich
Cumulus parameterizations	Grell 3
Chemistry option	Adopted scheme
Photolysis	Fast J
Gas-phase chemistry	RADM2
Aerosols	MADE/SORGAM
Anthropogenic emissions	NEI (2005)
Biogenic emissions	Guenther, from USGS land use classification

946

947

948 Table 3. Spatial Mean Fractional Bias (MFB) over the entire year. Recall

949
$$MFB = \frac{1}{N} \sum_1^N \frac{C_m - C_0}{\frac{C_m + C_0}{2}},$$
 where C_m is the monthly mean AOD or AE simulated by WRF-Chem

950 at a specific location and C_0 refers to the same quantity from MODIS/MISR/AERONET. Thus
 951 a negative value indicates the model is negatively biased relative to the observations. The total
 952 sample size N is 358,048 and 359,633 when comparing WRF-Chem with MODIS onboard
 953 Terra and Aqua respectively. The comparison between MODIS and AERONET is affected by
 954 a few outlier sites, so in parenthesis is the MFB when the three most biased sites are removed.
 955 The mean domain averaged AOD and AE from WRF-Chem (after applying the cloud screen
 956 and selecting only MODIS overpass hours) are 0.222 and 1.089, respectively.

Comparisons	MFB AOD	MFB AE
WRF-MODIS (Terra)	0. 20 <u>15</u>	-0.09
WRF-MODIS (Aqua)	0.14	-0.11
WRF-MISR (Terra)	0.16	-0.11
WRF-AERONET	0.50	-0.59
MODIS (Terra)-AERONET	-1.23 <u>(-0.91)</u>	-0.13 <u>(-0.11)</u>

957

958

959

960 Table 4. Contingency table used to compare the fraction of grid cells classified as fine ($AE >$
961 1) and coarse ($AE < 1$) by MODIS and WRF-Chem.

		MODIS	
		Fine	Coarse
WRF-Chem	Fine	WF/MF	WF/MC
	Coarse	WC/MF	WC/MC

962

963

964 Table 5. Contingency table showing the fraction of grid cells simultaneously identified as fine
 965 (WF/MF) or coarse (WC/MC) mode particles by WRF-Chem and MODIS, as well as cells with
 966 different classification (columns 4 and 5). Recall a threshold of AE = 1 is used to define fine
 967 (AE>1) and coarse mode (AE<1) dominance. Months in bold indicate the distribution of
 968 observed and simulated fine/coarse mode fractions are significantly different (p-value < 0.01)
 969 according to the χ^2 test described in Sect. 2.3.

Month	WF/MF	WC/MC	WF/MC	WC/MF
1	0.025	0.176	0.007	0.792
2	0.030	0.241	0.004	0.725
3	0.005	0.297	0.001	0.697
4	0.013	0.230	0.004	0.753
5	0.141	0.204	0.028	0.628
6	0.541	0.122	0.055	0.283
7	0.623	0.094	0.030	0.252
8	0.520	0.061	0.017	0.402
9	0.561	0.118	0.032	0.288
10	0.486	0.145	0.088	0.281
11	0.321	0.179	0.058	0.442
12	0.164	0.248	0.015	0.573
mean	0.286	0.176	0.028	0.510

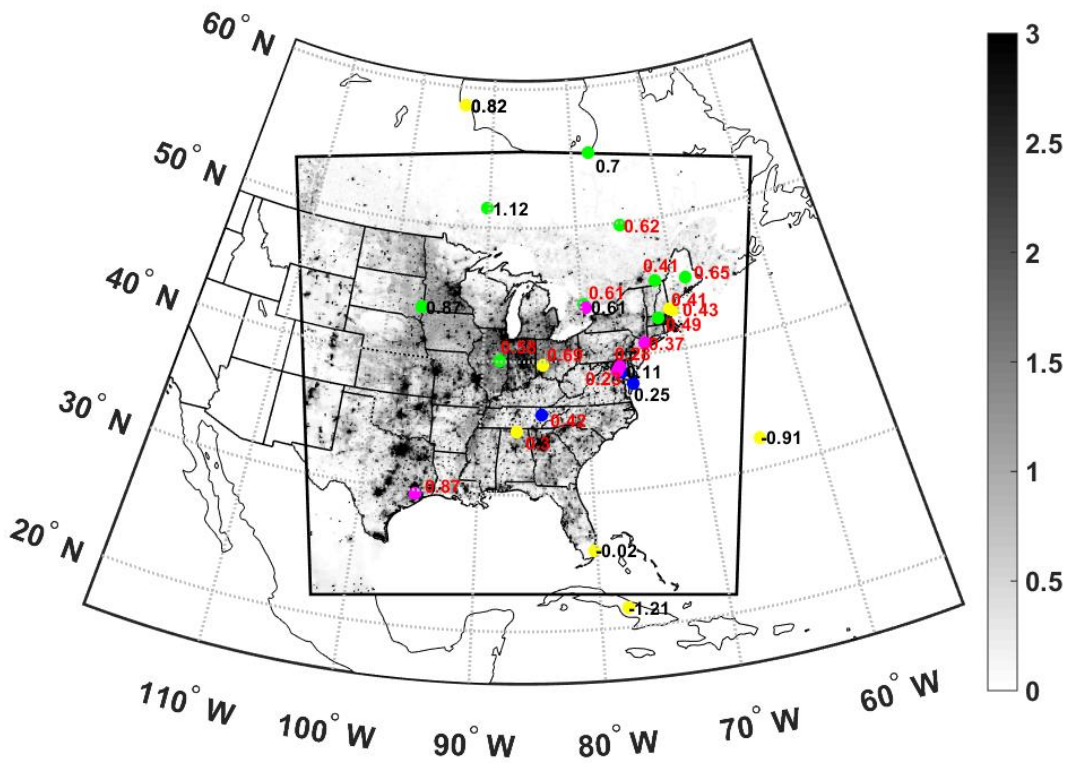
970

971

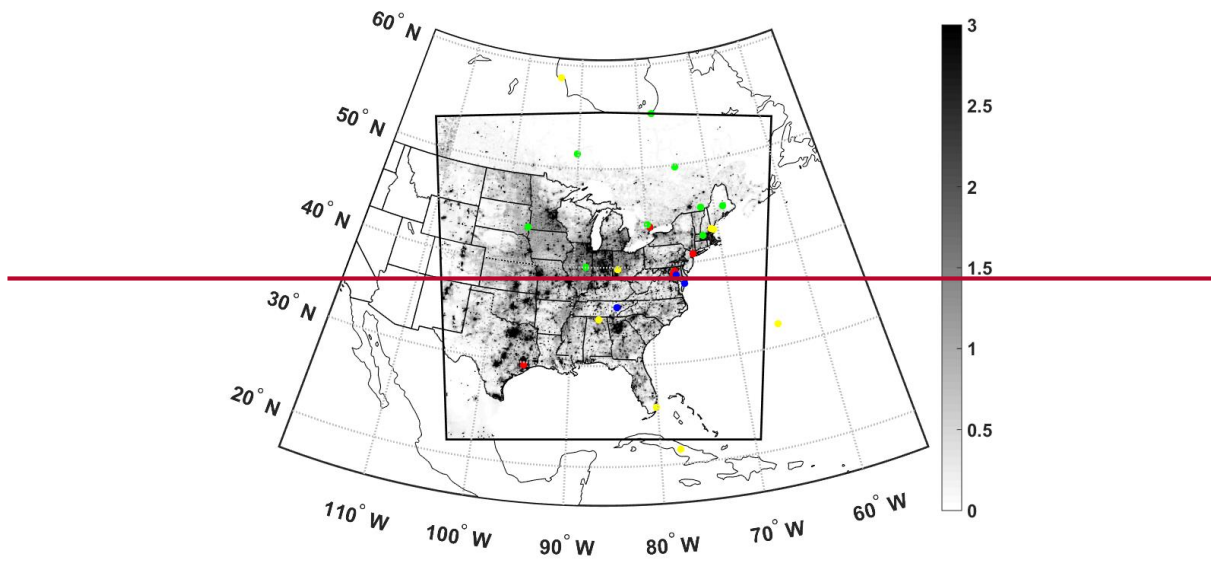
972 Table 6. Synthesis of the skill with which WRF-Chem identifies the spatial distribution and
 973 location of extreme AOD values. Cells with extreme AOD are identified as exceeding the 75th
 974 percentile computed on a monthly basis across space from monthly averaged daily means. The
 975 second column reports the Accuracy, which indicates the spatial coherence of extremes and
 976 non-extremes between WRF-Chem and MODIS. The Accuracy metric is computed as the sum
 977 of cells co-identified as exceeding the 75th percentile and not exceeding that threshold by WRF-
 978 Chem and MODIS (Terra) relative to the total number of cells with valid data (fifth column,
 979 *N*). The third column reports the Threat Score (*TS*) which indicates the probability of correctly
 980 forecasting extreme AOD conditional upon either forecasting or observing extremes. The fourth
 981 column shows the Hit Rate (*HR*) (i.e. probability of correct forecast), which is the proportion
 982 of cells correctly identified as extremes by WRF-Chem relative to MODIS extremes. Values in
 983 parenthesis refer to the same metrics when comparing WRF-Chem and MODIS onboard the
 984 Aqua satellite.

Month	Accuracy	TS	HR	N
Jan	0.664 (0.651)	0.196 (0.178)	0.328 (0.302)	14899 (15051)
Feb	0.654 (0.583)	0.182 (0.091)	0.308 (0.167)	13721 (13643)
Mar	0.656 (0.647)	0.185 (0.173)	0.312 (0.295)	16641 (16541)
Apr	0.645 (0.680)	0.169 (0.219)	0.289 (0.360)	25265 (24974)
May	0.664 (0.699)	0.196 (0.248)	0.327 (0.397)	32770 (31239)
Jun	0.796 (0.800)	0.420 (0.428)	0.592 (0.600)	36148 (34654)
Jul	0.850 (0.823)	0.538 (0.477)	0.700 (0.646)	36055 (35480)
Aug	0.834 (0.832)	0.500 (0.496)	0.667 (0.663)	39173 (39130)
Sep	0.667 (0.665)	0.200 (0.197)	0.333 (0.329)	35883 (35081)
Oct	0.656 (0.665)	0.185 (0.198)	0.311 (0.330)	29662 (26456)
Nov	0.703 (0.696)	0.254 (0.245)	0.405 (0.393)	21630 (19538)
Dec	0.648 (0.653)	0.173 (0.181)	0.295 (0.306)	14914 (14527)
Mean	0.703 (0.699)	0.266 (0.261)	0.406 (0.399)	26397 (25526)

985



987

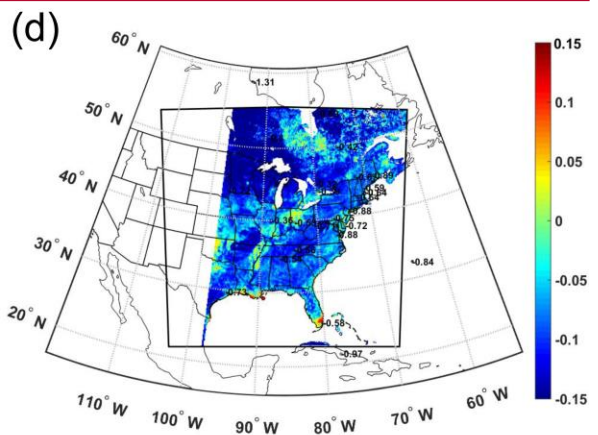
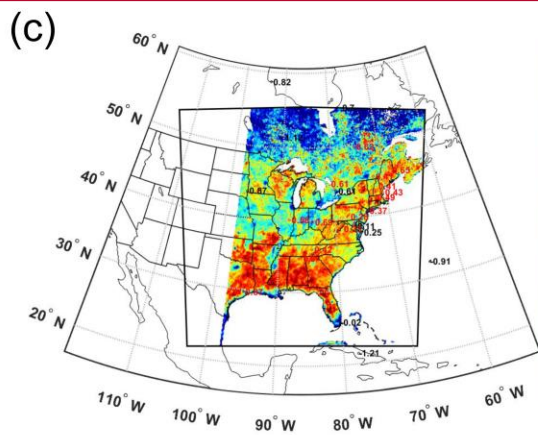
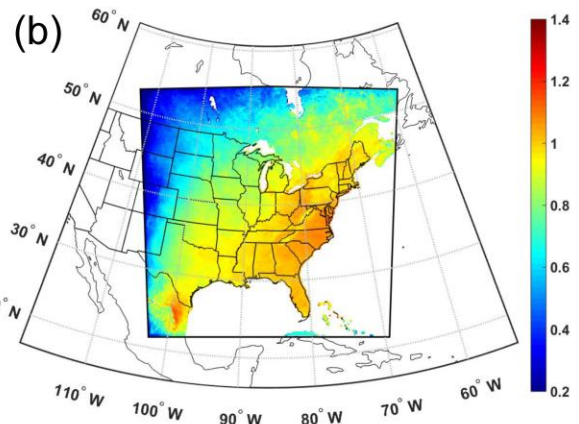
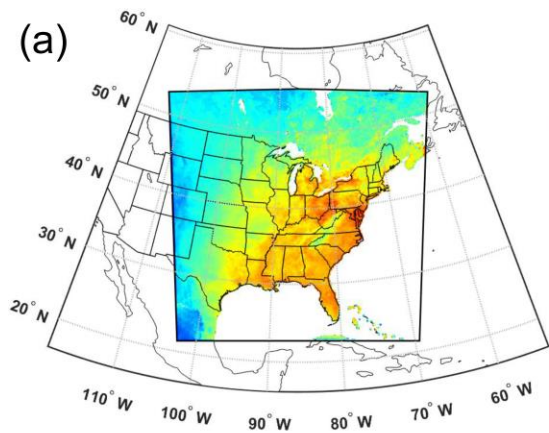


988

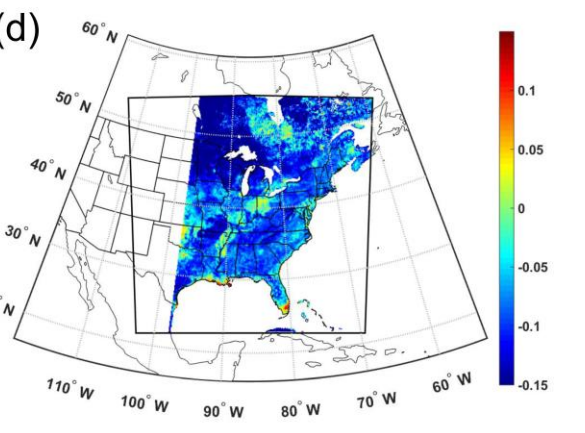
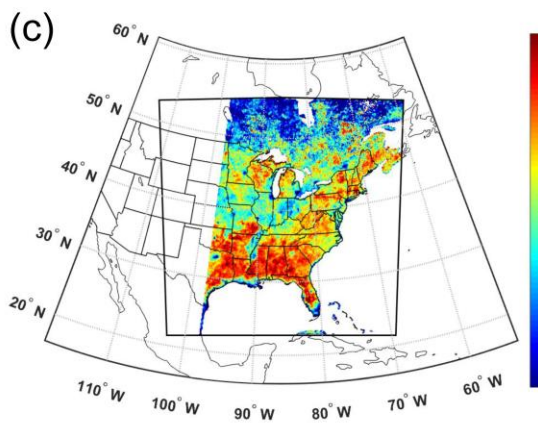
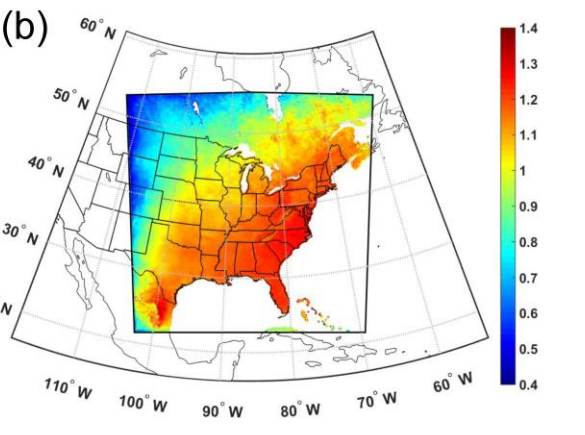
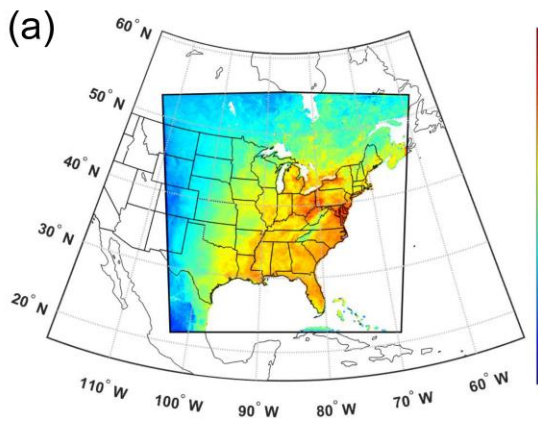
989

990 Figure 1. Location of the AERONET stations (colored dots) used in this study and mean daily
 991 PM_{2.5} emissions [$\text{mg m}^{-2} \text{day}^{-1}$] during 2008 (gray shading). Colors indicate the AERONET site
 992 classification based on (Kinne et al., 2013): polluted (~~red~~magenta), land (green), coastal (blue),
 993 un-classified (yellow). The numbers in panels c-d are MFB for WRF-Chem vs. AERONET

994 stations (red numbers indicate WRF-Chem vs. AERONET has a larger MFB than WRF-Chem
995 vs. MODIS whereas black numbers indicate a lower bias in the comparison with AERONET).



996

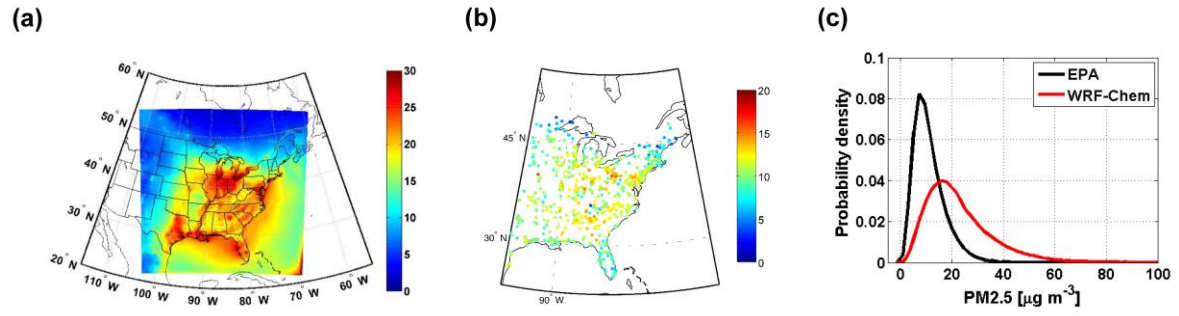
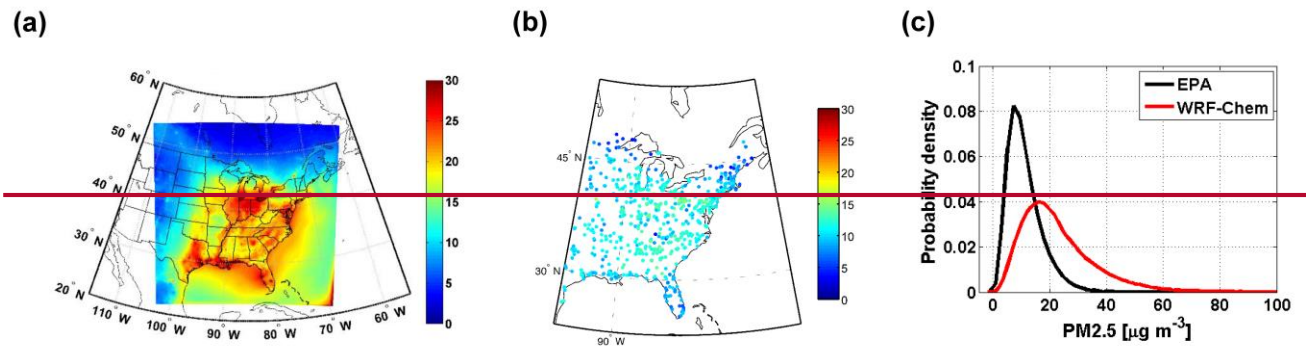


997

998

999 Figure 2. Mean (a) AOD and (b) AE simulated by WRF-Chem during the year 2008. The mean
1000 values are computed after applying a cloud mask and are for the Terra overpass time. Mean
1001 Fractional Bias (MFB) for (c) AOD and (d) AE for WRF-Chem relative to MODIS (Terra)
1002 (similar results are found for Aqua). ~~The numbers in panels c-d are MFB for WRF-Chem vs~~
1003 ~~AERONET stations (red numbers indicate WRF-Chem vs. AERONET has a larger MFB than~~
1004 ~~WRF-Chem vs. MODIS whereas black numbers indicate a lower bias in the comparison with~~
1005 ~~AERONET).~~ The inner black frame indicates the entire model domain, while as stated in the
1006 text model evaluation is only undertaken for longitudes east of 98°W.

1007



1008

1009

1010

1011

1012

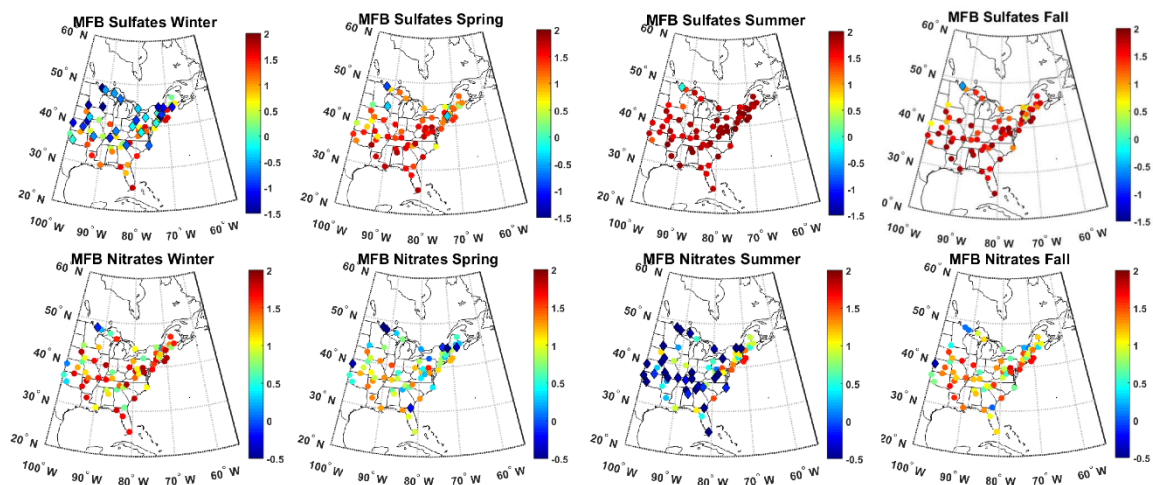
1013

1014

1015

Figure 3. Mean daily PM_{2.5} concentrations [$\mu\text{g m}^{-3}$] during 2008 as (a) simulated by WRF-Chem in the layer closest to the surface and (b) observed at 1230 EPA sites (note the different colorbar). Panel (c) shows the probability distribution of daily mean PM_{2.5} concentrations observed (black line) and simulated (red line) at the measurement stations.

1016
1017
1018
1019
1020
1021
1022
1023
1024
1025
1026

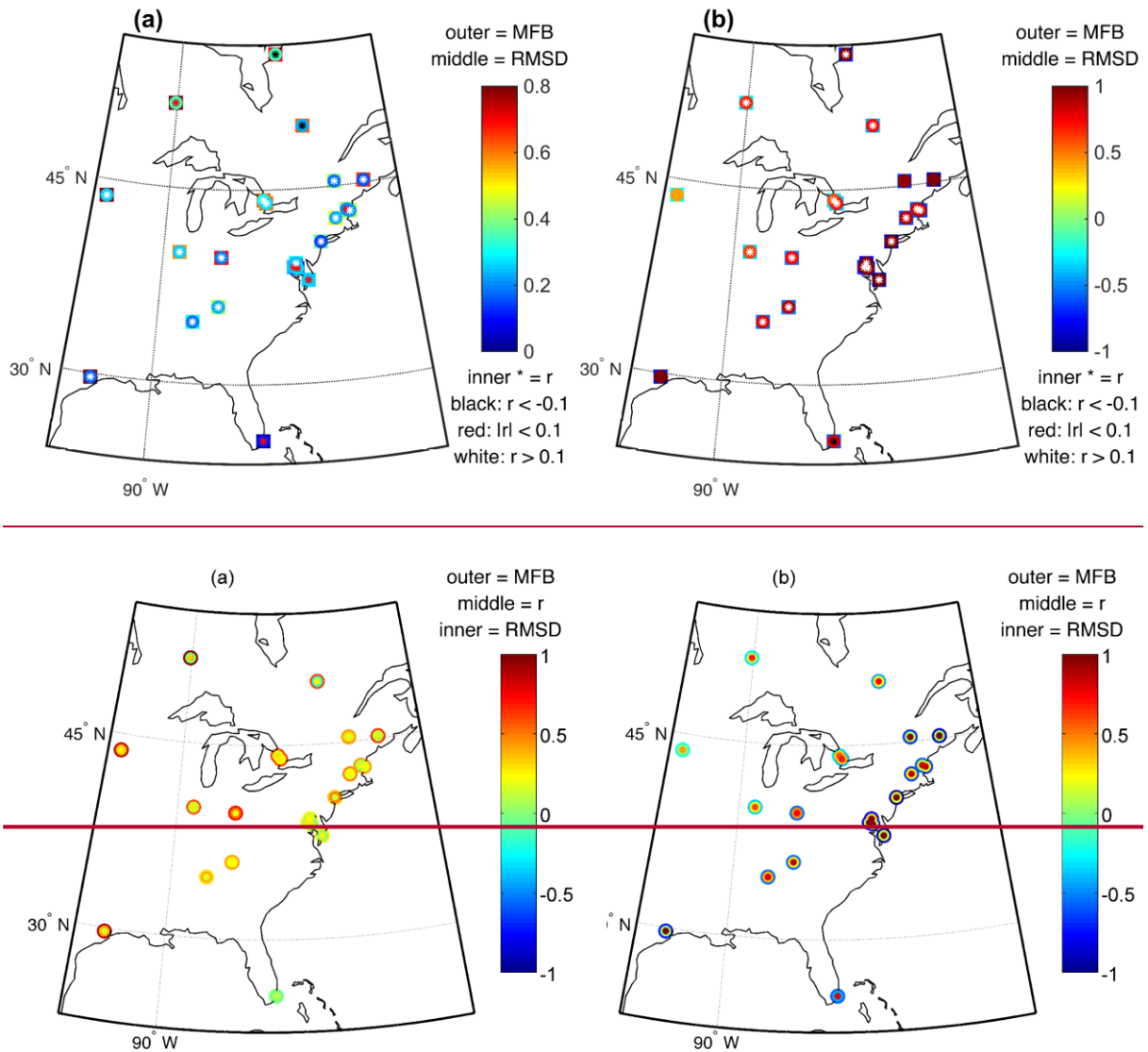


1027
1028
1029
1030
1031
1032
1033
1034

Figure 4. Mean fraction bias (MFB) of near-surface daily mean sulfate (first line) and nitrate (second line) concentrations in fine aerosol particles as simulated by WRF-Chem and observed in PM_{2.5} measurements at 123 IMPROVE sites in different seasons. A positive MFB indicates WRF-Chem overestimates the observations. Note the scales differ between the frames shown for sulfate and nitrate MFB and dots/diamonds refer to positive/negative MFB.

1035

1036



1037

1038

1039

1040 Figure 45. Summary statistics of comparisons of WRF-Chem simulations of (a) AOD and (b)
 1041 AE relative to simultaneous observations at the AERONET sites. For a location to be included
 1042 in this analysis at least 20 coincident observations and simulations must be available. The
 1043 symbols at each AERONET station report MFB (outer ~~circle~~ square), root mean squared
 1044 difference (RMSD, ~~correlation coefficient (r)~~ middle inner circle) and correlation coefficient
 1045 (~~r~~, root mean squared difference (RMSD) (inner *)). Note the different colorbar for MFB and
 1046 RMSD between the two frames. The correlation coefficient is displayed with different colors

1047 according with 3 classes: $r < -0.1$ (black), $|r| < 0.1$ (red) and $r > 0.1$ (white). ~~Note: For a location~~
1048 ~~to be included in this analysis at least 20 coincident observations and simulations must be~~
1049 ~~available.~~
1050

1051
|
1052

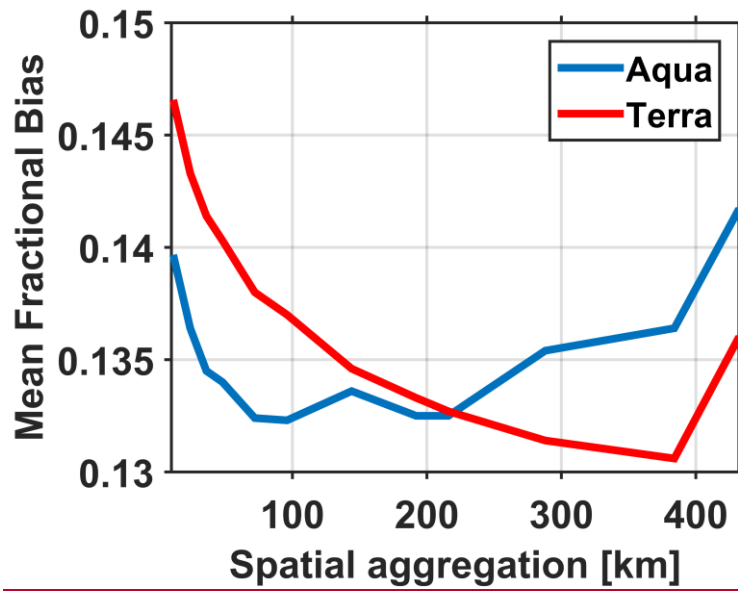
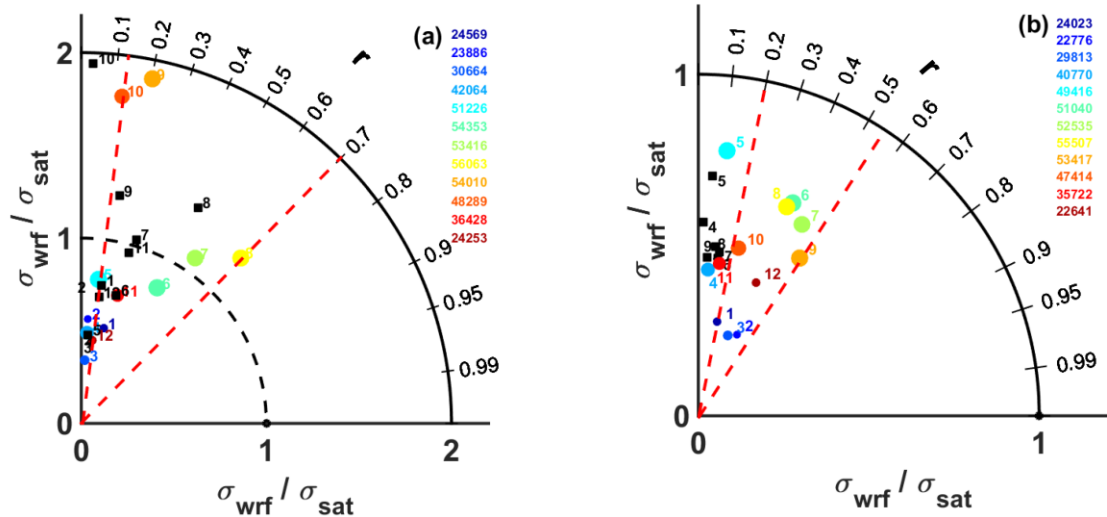


Figure 6. Mean Fractional Bias (MFB) on AOD from WRF-Chem as a function of spatial aggregation relative to observations from Terra (red line) and Aqua (blue line).

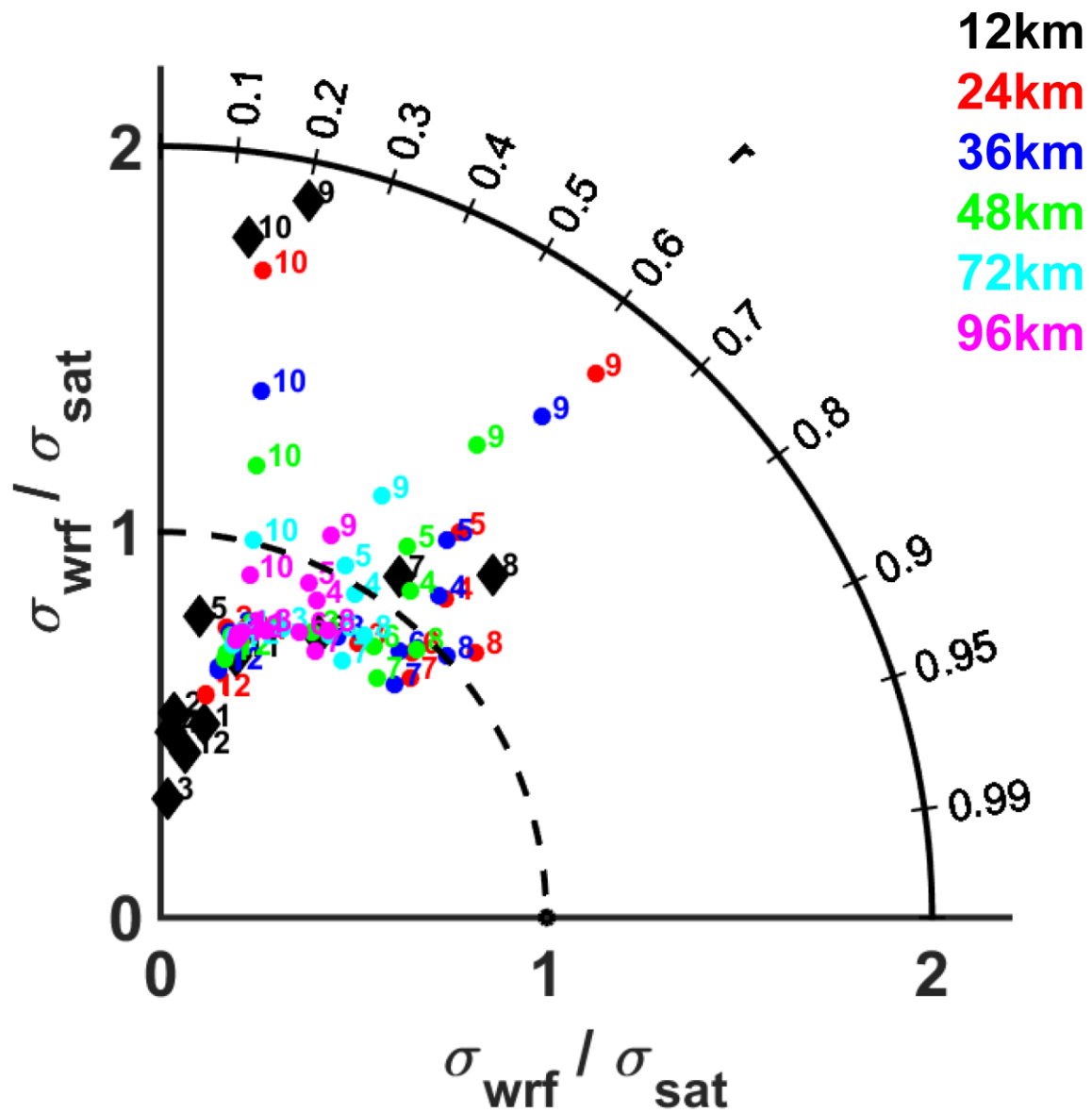
1053
1054
1055
1056
1057
1058
1059
1060
1061
1062
1063
1064
1065
1066
1067
1068
1069
1070



1071

1072 Figure 7. Taylor diagrams comparing the spatial fields of monthly mean (a) AOD and (b) AE
 1073 from WRF-Chem vs MODIS-Terra (color dots) or MISR (black squares). The numbers shown
 1074 in the frames denote the month (e.g. 1 = Jan). The numbers shown in the legend indicate
 1075 the sample size of WRF-Chem data used for computing the monthly mean and the scale of the dots
 1076 is proportional to the sample size. Note the change in scale for the ratio of standard deviations
 1077 between the frames. The red dashed lines define the sector with Pearson correlation coefficient
 1078 between (a) 0.12-0.70 for AOD and (b) 0.20-0.54 for AE which comprise at least two thirds of
 1079 the months. Each dot/square summarizes the statistics (i.e. RMSD, ratio of standard deviations
 1080 and correlation coefficient) of the WRF-Chem vs MODIS/MISR comparison for a single
 1081 month.

1082



1083

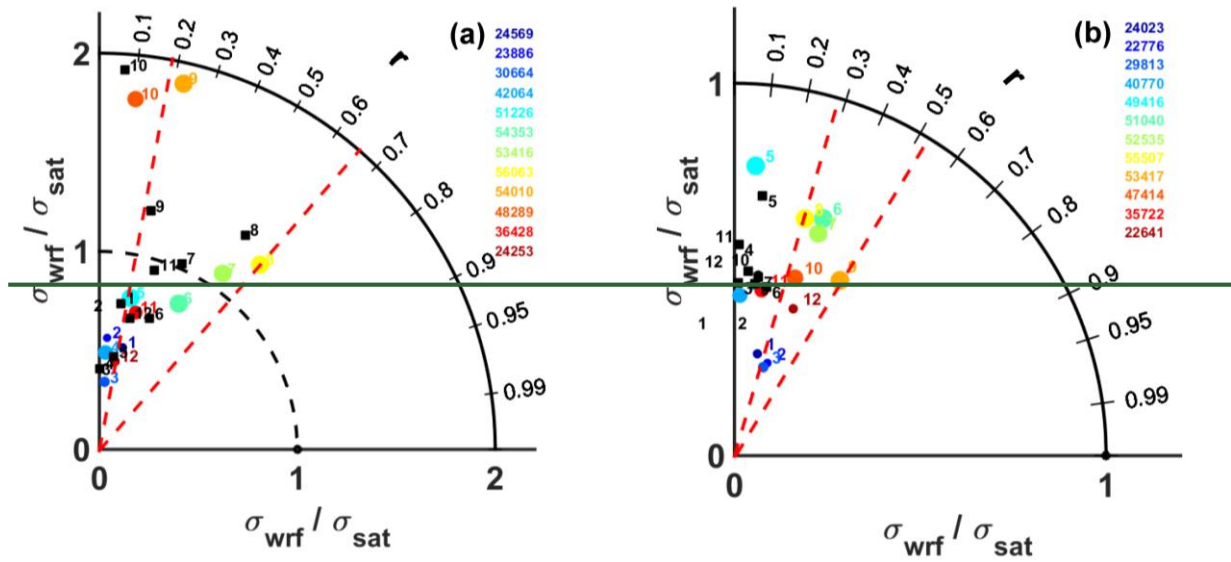
1084 Figure 8. Taylor diagrams for AOD when MODIS observations and WRF-Chem simulations

1085 at 12 km are spatially aggregated to 24, 36, 48, 72 and 96 km. Numbers next to the colored

1086 dots/diamonds indicate different months (e.g. 1 = Jan).

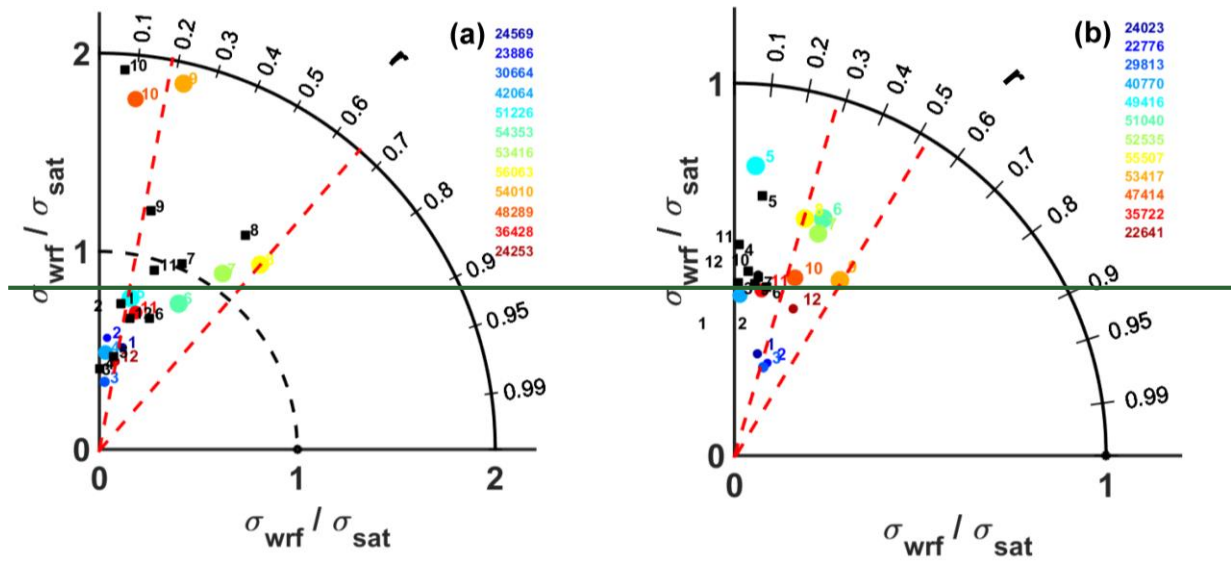
1087

1088
1089



1090
1091
1092
1093
1094
1095
1096
1097
1098
1099
1100
1101
1102
1103

Figure 5. Taylor diagrams comparing the spatial fields of monthly mean (a) AOD and (b) AE from WRF-Chem vs MODIS-Terra (color dots) or MISR (black squares). The numbers shown in the frames denote the month (e.g. 1 = Jan). The numbers shown in the legend indicate the sample size of WRF-Chem data used for computing the monthly mean and the scale of the dots is proportional to the sample size. Note the change in scale for the ratio of standard deviations between the frames. The red dashed lines define the sector with Spearman's rank correlation coefficient between (a) 0.18-0.66 for AOD and (b) 0.28-0.52 for AE which comprise at least two thirds of the months. Each dot/square summarizes the statistics (i.e. RMSD, ratio of standard deviations and correlation coefficient) of the WRF-Chem vs MODIS/MISR comparison for a single month.



1104

1105

1106

1107

1108

1109

1110

1111

1112

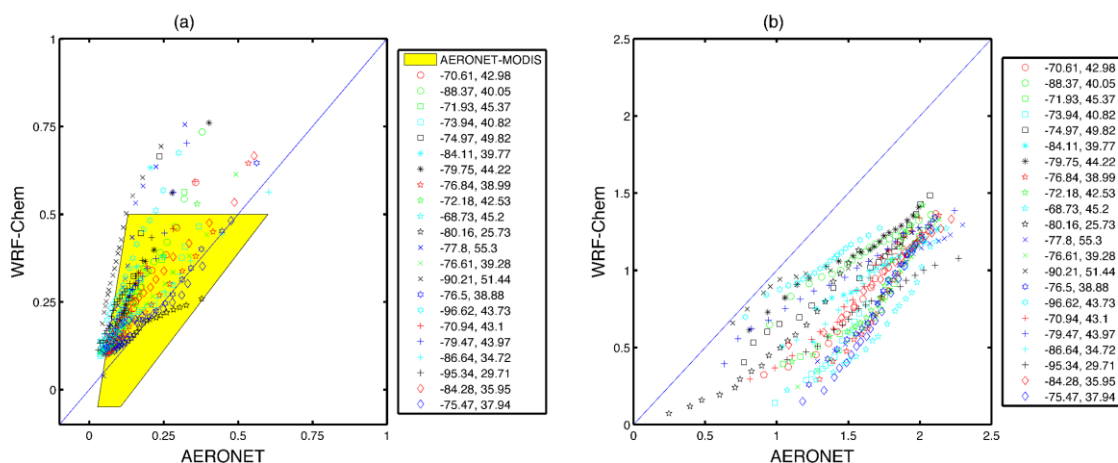
1113

1114

1115

1116

Figure 5. Taylor diagrams comparing the spatial fields of monthly mean (a) AOD and (b) AE from WRF-Chem vs MODIS-Terra (color dots) or MISR (black squares). The numbers shown in the frames denote the month (e.g. 1 = Jan). The numbers shown in the legend indicate the sample size of WRF-Chem data used for computing the monthly mean and the scale of the dots is proportional to the sample size. Note the change in scale for the ratio of standard deviations between the frames. The red dashed lines define the sector with Spearman's rank correlation coefficient between (a) 0.18-0.66 for AOD and (b) 0.28-0.52 for AE which comprise at least two thirds of the months. Each dot/square summarizes the statistics (i.e. RMSD, ratio of standard deviations and correlation coefficient) of the WRF-Chem vs MODIS/MISR comparison for a single month.

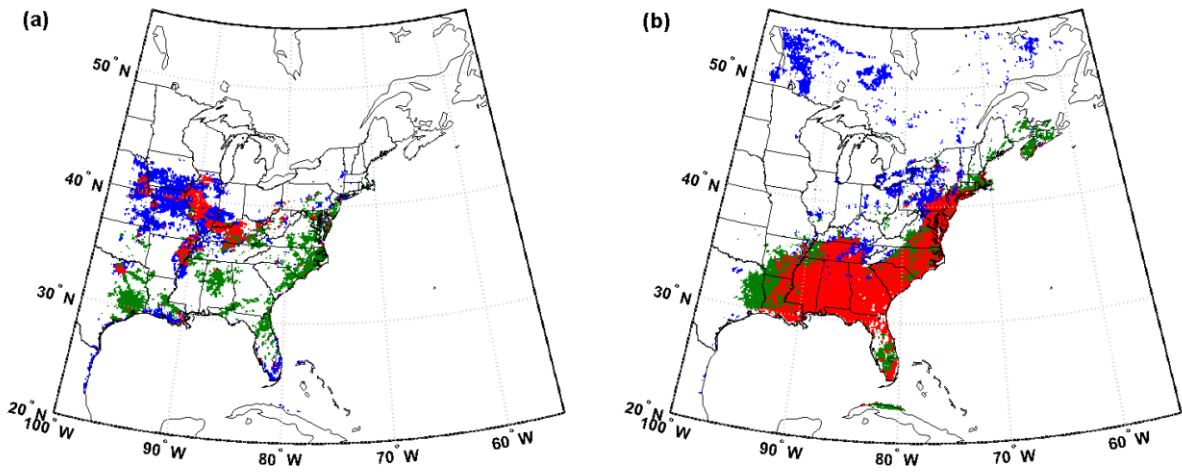


1118

1119

1120 Figure 69. Empirical quantile-quantile (EQQ) plots of (a) AOD and (b) AE of the 5th to 95th
 1121 percentile as simulated by WRF-Chem relative to 22 AERONET stations (their longitude (E)
 1122 and latitude (N) is reported in the legend). The yellow shading shows the data envelope for
 1123 EQQ plots of AERONET and MODIS. For inclusion in the analysis a location must have at
 1124 least 20 coincident observations and simulations in the grid cell containing the AERONET
 1125 station. Note MODIS uncertainty in the retrievals (± 0.05) in near zero AOD conditions may
 1126 lead to negative AOD values which are considered valid. The parameter space for MODIS-
 1127 AERONET comparisons of AE are not shown because AE from the MODIS L2 data product
 1128 are strongly bimodal (see examples given in Fig. 1 in the Supplementary Materials).

1129

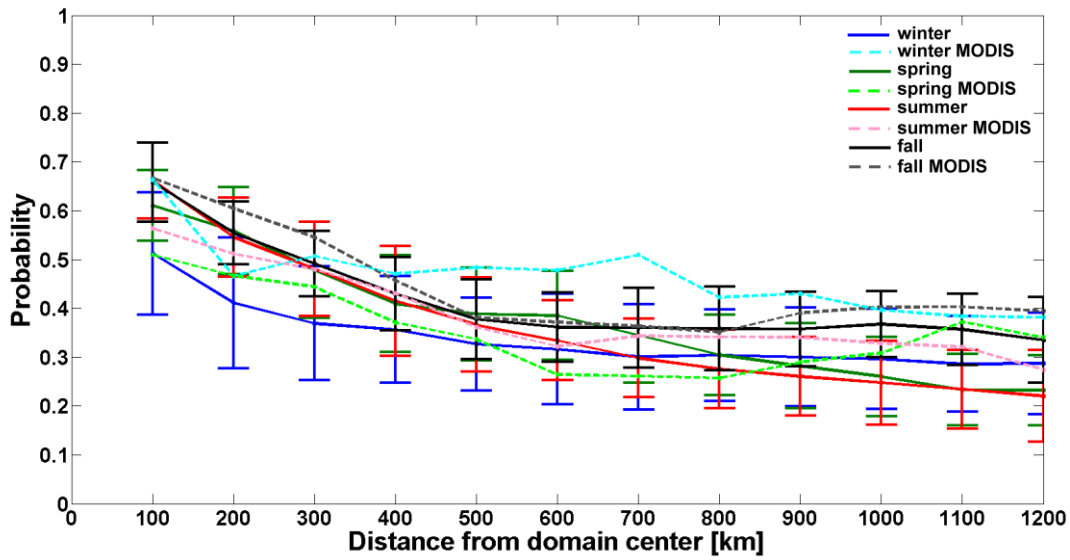


1130

1131

1132 Figure 710. Spatial coherence in extreme AOD (i.e. the occurrence of AOD above the 75th
 1133 percentile value) from WRF-Chem and MODIS Terra during (a) March (03/2008) and (b) July
 1134 (07/2008). Green areas denote grid cells defined as experiencing extreme AOD only in the
 1135 WRF-Chem simulations, blue pixels indicate extreme values as diagnosed using MODIS, while
 1136 red pixels indicate areas where the occurrence of extreme values is indicated by both the WRF-
 1137 Chem simulations and the MODIS observations.

1138



1140

1141

1142 Figure 811. Mean and error bars (± 1 standard deviation from the mean) of the probability of
 1143 co-occurrence of extreme AOD (i.e. AOD > 75th percentile) at the reference location (i.e.
 1144 domain center) and any other simulated grid cell during different seasons. The distance between
 1145 the reference point and each grid cell centroid was binned using 100 km distance classes. Solid
 1146 lines indicate mean seasonal spatial scales simulated by WRF-Chem, whereas dashed lines are
 1147 observed means from L2 MODIS data (only the mean of the coherence ratios is plotted for the
 1148 MODIS data).

1149